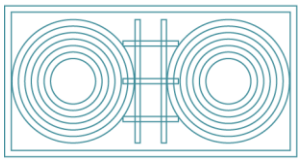

DEHLSEN ASSOCIATES, LLC

Final Technical Report

Advanced Controls for the Multi-pod Centipod WEC device

DE-EE0006404

Dec 2013 - Oct 2015

15 Feb 2016

Principle Investigator:
Alex Fleming, CTO
afleming@ecomerittech.com
805-845-9100

Report Author:
Alan McCall, Mechanical Engineer
amccall@ecomerittech.com
805-845-0496

Dehlsen Associates, LLC
101 E. Victoria Street, Suite F, Santa Barbara, CA 93101

Working Partners:
Dr. Ted Brekken
Mike Starrett
Ratanak So
Oregon State University
brekken@eecs.oregonstate.edu
541-737-2995

Jarett Goldsmith
DNV GL - Energy
Jarett.Goldsmith@dnvgl.com
858-836-3370

Dr. Sandeep Gupta
Helios Engineering Inc.
sgupta@heliosengineeringinc.com
805-701-8506

U.S. Department of Energy Disclaimer

This report was prepared as an account of work partially sponsored by an agency of the United States Government. Neither the United States Government nor any agency thereof, nor any of their employees, makes any warranty, express or implied, or assumes any legal liability or responsibility for the accuracy, completeness, or usefulness of any information, apparatus, product, or process disclosed, or represents that its use would not infringe privately owned rights. Reference herein to any specific commercial product, process, or service by trade name, trademark, manufacturer, or otherwise does not necessarily constitute or imply its endorsement, recommendation, or favoring by the United States Government or any agency thereof. The views and opinions of authors expressed herein do not necessarily state or reflect those of the United States Government or any agency thereof.

Project Consortium Legal Notice/Disclaimer

This report was prepared by Dehlsen Associates, LLC pursuant to a Grant funded by the U.S. Department of Energy (DOE) under Instrument Number DE-EE0006404 NO WARRANTY OR REPRESENTATION, EXPRESS OR IMPLIED, IS MADE WITH RESPECT TO THE ACCURACY, COMPLETENESS, AND/OR USEFULNESS OF INFORMATION CONTAINED IN THIS REPORT. FURTHER, NO WARRANTY OR REPRESENTATION, EXPRESS OR IMPLIED, IS MADE THAT THE USE OF ANY INFORMATION, APPARATUS, METHOD, OR PROCESS DISCLOSED IN THIS REPORT WILL NOT INFRINGE UPON PRIVATELY OWNED RIGHTS. FINALLY, NO LIABILITY IS ASSUMED WITH RESPECT TO THE USE OF, OR FOR DAMAGES RESULTING FROM THE USE OF, ANY INFORMATION, APPARATUS, METHOD OR PROCESS DISCLOSED IN THIS REPORT.

NOTE:

For further information about Dehlsen Associates, LLC, call 805-845-7575 or e-mail Alex Fleming at afleming@ecomerittech.com.

This publication is a corporate document that should be cited in the literature in the following manner: " Advanced Controls for the Multi-pod Centipod WEC device". Dehlsen Associates, LLC, Santa Barbara, CA and U.S. Department of Energy, Washington, DC. 2016.

This report describes research sponsored by Dehlsen Associates and the U.S. Department of Energy. The U.S. Department of Energy, Energy Efficiency and Renewable Energy Office, Wind & Water Power Program provided 80% of project funding via grant number DE-EE0006404, "Advanced Controls for the Multi-pod Centipod WEC device". Long-term development of the Centipod Wave Energy Converter including the accomplishments discussed herein would not have been possible without the support and vision of many DOE project managers.

Table of Contents

1.0 Contractual Information 5
2.0 Executive Summary 6
3.0 Proposed Project Parameters 6
3.1 Project Objectives 6
3.2 Project Scope 6
3.3 Tasks to be Performed 7
4.0 Project Organization 10
5.0 Project Task Activities 11
5.1 Task 1.0 - Develop reduced model representation for Centipod 11
5.2 Task 2.0 - Develop baseline global integration model in WaveDyn 14
5.2.1 Hydrodynamics Data 14
5.2.2 WaveDyn Model 17
5.3 Task 3.0 - Baseline performance and operational loads calculations 19
5.3.1 Performance Calculation 19
5.3.1.1 Baseline Controller 19
5.3.1.2 Power Matrix Methodology 19
5.3.1.3 AEP Calculation 20
5.3.2 Operational Loads 20
5.3.2.1 Methodology 20
5.3.2.1 Results 20
5.4 Task 4.0 - Develop model predictive control framework 21
5.4.1 Controller Overview 21
5.4.2 Kalman Estimator 21
5.4.3 Fe Prediction 22
5.4.4 MPC 24
5.4.5 Constraints 24
5.5 Task 5.0 - MPC performance and operational loads calculation 25
5.5.1 Performance Calculation 25
5.5.1.1 Implementation of MPC 25
5.5.1.2 Power Matrix Methodology 25
5.5.1.3 AEP Calculation 25
5.5.2 Operational Loads 27
5.5.2.1 Methodology 27
5.5.2.1 Results 27
5.6 Task 6.0 - Extreme sea state load calculations 29
5.6.1 Methodology 29
5.6.2 Baseline vs. MPC 34
5.7 Task 7.0 - Perform impact analysis 35
5.7.1 LCOE 35
5.7.1.1 Cost of the Machine 36
5.7.1.2 Balance of System 38
5.7.2 AEP 39
5.7.3 PWR 40
5.7.4 Summary of Metrics 40

5.8 Task 8.0 - Design real-time implementation of MPC controller 40
6.0 Accomplishments 42
7.0 Conclusions 42
8.0 References 43

1.0 Contractual Information

Federal Agency to which Report is submitted: DOE EERE – Wind & Water Power Program

Recipient: Dehlsen Associates, LLC - DUNS 830226317
Award Number: DE-EE0006404
Project Title: Advanced Controls for the Multi-pod Centipod WEC device
Project Period: Dec 1 2013 to Oct 31, 2015

Principle Investigator: Alex Fleming, VP of Engineering, afleming@ecomerittech.com; 101 E. Victoria Street, Suite F, Santa Barbara, CA 93101; 805-845-9100

Report Submitted by: Dave Arthurs, CFO, darthurs@ecomerittech.com; 101 E. Victoria Street, Suite F, Santa Barbara, CA 93101; 805-845-9101

Date of Report: Feb 15, 2016

Covering Period: Dec 1 2013 to Oct 31, 2015

Working Partners:
Ted Brekken
Oregon State University
brekken@eecs.oregonstate.edu
541-737-2995

Jarett Goldsmith
DNV GL - Energy
Jarett.Goldsmith@dnvgl.com
858-836-3370

Dr. Sandeep Gupta
Helios Engineering Inc.,
sgupta@heliosengineeringinc.com
805-701-8506

Cost-Sharing Partners: N/A

DOE Project Team: DOE HQ Program Manager – Jose Zayas
DOE Field Contract Officer – Pamela Brodie
DOE Field Grants Management Specialist – Yvette Peterson
DOE Field Project Officer – Tim Ramsey
DOE/CNJV Project Monitor – Michael Carella

Signature of Submitting Official: _____
(electronic signature is acceptable)

2.0 Executive Summary

Dehlsen Associates, LLC (DA) has developed a Wave Energy Converter (WEC), Centipod, which is a multiple point absorber, extracting wave energy primarily in the heave direction through a plurality of point absorber floats sharing a common stable reference structure. The objective of this project was to develop advanced control algorithms that will be used to reduce Levelized Cost of Energy (LCOE). This project investigated the use of Model Predictive Control (MPC) to improve the power capture of the WEC.

The MPC controller developed in this work is a state-space, "look ahead" controller approach using knowledge of past and current states to predict future states to take action with the PTO to maximize power capture while still respecting system constraints. In order to maximize power, which is the product of force and velocity, the controller must aim to create phase alignment between excitation force and velocity.

This project showed a 161% improvement in the Annual Energy Production (AEP) for the Centipod WEC when utilizing MPC, compared to a baseline, fixed passive damping control strategy. This improvement in AEP was shown to provide a substantial benefit to the WEC's overall Cost of Energy, reducing LCOE by 50% from baseline. The results of this work proved great potential for the adoption of Model Predictive Controls in Wave Energy Converters.

3.0 Proposed Project Parameters

3.1 Project Objectives

Dehlsen Associates, LLC (DA) proposed to develop innovative advanced control algorithms to optimize power production and dynamic loads for the multi-pod Centipod Wave Energy Converter (WEC) utilizing a novel energy efficient PTO system. The scope and tasking for this project, as written in the original Statement of Project Objectives (SOPO) is described below.

3.2 Project Scope

Dehlsen Associates, LLC (DA) has developed a novel concept, Centipod, which has evolved from extensive research and several rounds of prototype testing to arrive at a design which shows significant improvements in the area of material usage. The objective of this project was to develop advanced control algorithms that will be used to further reduce Levelized Cost of Energy (LCOE), improve Power-to-Weight Ratio (PWR) for Centipod and achieve DOE Wind and Water Power Technologies Office's Water Program's goal of performance enhancement of Marine Hydrokinetic (MHK) devices.

This project investigated the use of Model Predictive Control (MPC) to improve the power capture and reduce design loads for the MHK device. Real time implementation of such algorithms was also to be evaluated. In addition, control algorithms were developed for the survival system or detuning for an extreme sea state with the pod feathering mechanism on Centipod.

3.3 Tasks Performed

Task 1.0 Develop reduced model representation for Centipod

Milestones: Validation of reduced order model.

Deliverables: Reduced order model, performance results for reference site.

Subtask 1.1. Reduced model for single pod and Power Take Off (PTO)

Develop a reduced order model for single pod and PTO to create the plant model. ANSYS AQWA, or similar Software tool will be used to estimate hydrodynamic parameters in frequency domain. Results from this simple model will be compared against Dehlsen Associates previous work on pod optimization and geometry.

Subtask 1.2. Reduced model for multi pod Centipod

Develop a reduced order model for Centipod with multiple pods, PTO and the backbone. Simulations will be performed assuming no interference of pods. Hydrodynamic models will then be developed to account for interference between pods and results compared with the former. The boundary conditions will be based on likely deployment test sites and target commercial sites.

Subtask 1.3. Performance calculations and validation

Use the reduced order models and calculate performance at the site with basic controller and passive damping. These will be used as baseline results to compare against calculations resulting from task 3, carried out in parallel with this effort to perform validation of the reduced order model.

Task 2.0 Develop baseline global integration model in WEC performance and loading design software (WaveDyn or similar)

Milestones: Global integration model for Centipod.

Deliverables: Fully integrated model of Centipod.

Subtask 2.1. Obtain hydrodynamic data for wetted geometry

Obtain hydrodynamic data for geometry using a wave analysis flow solver. The wetted geometry will be meshed in the MultiSurf surface modeling CAD package. Convergence studies will be performed using mesh refinement in MultiSurf. The flow solver data will be post-processed, to dimensionalize the flow solver data to derive the input hydrodynamic information for the global integration model.

Subtask 2.2. Build system model of Centipod using WEC performance and loading design software

Build a system model of the machine, including the backbone, pods, and PTO components. Hydrodynamics components will be attached to the backbone and pods, allowing the processed hydrodynamic properties to be incorporated. PTO will be defined that meets the target PTO characteristics. Parametric studies involving advanced controls to optimize PTO topologies will be explored. Mooring lines will be modeled as quasi-static. Stability and robustness tests on the model using a neutral control setting will be run.

Task 3.0 Baseline performance and operational loads calculations in WEC performance and loading design software

Milestones: Benchmark baseline performance and loads.

Deliverables: Performance results, Operational load calculation report.

Subtask 3.1. Performance calculation

Develop comprehensive performance assessment data set for Centipod. Irregular wave simulations covering phase and spectral variability would be run using measured or standard shape spectral data. Power capture will be derived; in particular, a power matrix for the device (either using specific site data or a utilizing a generic spectral shape) will be derived.

Subtask 3.2. Operational loads calculation

Simulate operational loads either using specific site data or a utilizing a generic spectral shape. PTO loading and system loads baseline will be established.

Subtask 3.3. Baseline performance and loads report

Generate a performance and loads report that will serve as a baseline for comparison purposes. This report will not include extreme loads but only operational loads.

Task 4.0 Develop model predictive control framework

Milestones: Deliver Simulink model for MPC controller.

Deliverables: Simulink controller model, Simulation results with MPC.

Subtask 4.1. Develop cost function and constraints

Develop a cost function that needs to be minimized or maximized using model predictive control based on performance and loads calculations available. Constraints that drive the system cost (e.g. generator force, heave velocity etc.) will be specified to add to the model. Perform Techno-economic model that optimizes between advanced controls, PTO, subsystems, reliability, efficiency, operations and maintenance for a 20 year design life.

Subtask 4.2. Incorporate and validate wave prediction algorithm

Model wave predicting algorithms using adaptive least square or extended Kalman filter based methods will be investigated and the most appropriate method will be used. Accuracy will be traded against computational complexity. These algorithms will then be validated using the wave data available for regular and irregular waves.

Subtask 4.3. Develop model predictive control in Simulink

Create model predictive control algorithm and simulate in Simulink. Based on results from earlier tasks, a simplified model (with no pod interaction) will be used if the results indicate that there is no substantial difference in controller response for the device with and without modeling interaction. Performance calculations will be performed either using site data or a utilizing a generic spectral shape and MPC tuned based on the cost function and results compared with baseline controller.

Task 5.0 MPC performance and operational loads calculation

Incorporate MPC into global integration model and simulate performance and operational loads calculations. Perform optimization studies with different cost functions.

Milestones: Complete analysis of MPC controller versus baseline

Deliverables: Fully integrated MPC controller in WEC performance and loading design software, Performance and operational loads results.

Subtask 5.1. Incorporate MPC controller in WEC performance and loading design software

Incorporate MPC controller in WEC performance and loading design software. The WEC performance and loading design software will communicate with external controller using a Windows DLL. Simulink controller model will be re-programmed in C to create Windows DLL. After linking the controller DLL with WaveDyn, validation runs will be done to compare results against Simulink/AQWA model.

Subtask 5.2. Performance and loads calculations with MPC controller

Simulate performance and operational loads for the same set of conditions either using specific site data or a utilizing a generic spectral shape. Results will be investigated to ensure that the specified constraints are met and performance and operational loads compared against baseline results. Simulations will be benchmarked to record the computational time required on a desktop computer and estimates for state of the art embedded processors.

Subtask 5.3. Optimization of MPC algorithm

An optimization study will be performed using various cost functions and constraint for MPC. Additionally, a hardware unconstrained case will be explored. This will demonstrate the power of MPC framework and online optimization to account for various constraints as may be applicable for different kind of devices as well as the potential outside of existing technology. Two different scenarios will be looked at (1) Power maximization (2) Loads minimization.

Task 6.0 Extreme sea state load calculations in WEC performance and loading design software

Milestones: Development of Centipod "extreme condition response" controls

Deliverables: Extreme loads reduction report with advanced controls

Subtask 6.1. Create extreme sea state condition matrix

Dehlsen Associates will create the extreme sea state conditions based on either site-specific data or based on DNV standard to calculate extreme loads on Centipod.

Subtask 6.2. Perform Simulation under Extreme Conditions

Use the system integration model built in Task 1 to simulate the load cases under extreme sea state for pitching and non-pitching pods.

Subtask 6.3. Optimization of extreme response controls with MPC

Investigate the use of MPC to optimize controls under extreme sea state conditions.

Task 7.0 Perform impact analysis

Use loads results of the simulation to update design and calculate new SPA metrics.

Milestones: Updated design of Centipod device.

Deliverables: Finite element analysis reports, weights and cost spreadsheets

Subtask 7.1. Perform structural design iteration with updated loads

Perform finite element analysis in ANSYS/NASTRAN for the backbone structure, pods and heave plates with updated loads from performance modeling results. PTO design will be updated to reflect reduced requirements of force and heave velocity.

Subtask 7.2. Updated PWR and Availability Metrics

Update complete analysis of the stated FOA metrics of PWR and Availability using performance calculations for MPC controller and device weight with updated loads. Compare the results to baseline controller.

Task 8.0 Design real-time implementation of MPC controller

Implement advanced convex optimization techniques to develop a real-time MPC controller.

Milestones: Controller benchmarking with and without convex optimization

Deliverables: Controller code in C or MATLAB with convex optimization, hardware requirements for MPC implementation

Subtask 8.1. Implement convex optimization coding for MPC

Investigate the convex optimization techniques and decide on the best implementation strategy. Implement the chosen strategy in CVXGEN (convex optimization auto-coder from Stanford) or a similar tool to get a C-code or MATLAB mex function for Simulink analysis.

Subtask 8.2. Benchmark speed-up with convex optimization

Simulate selected cases with the MPC controller with and without the convex optimization code to benchmark speed-up of online optimization and evaluate if the speed-up is sufficient for real-time implementation. Based on these results, hardware requirements (processor speed, cache, memory) will be defined for system integration into Centipod.

4.0 Project Organization

Dehlsen Associates took on this project with the support of working partners with expertise in both control system development and numerical modeling of Wave Energy Converters. Oregon State University and Helios Engineering were the leading working partners in the domain of control system development within this project, providing leadership and experience to the development of the model predictive framework. Meanwhile DNV GL led the numerical modeling effort through the application of their commercial WEC analysis tool, WaveDyn. The National Renewable Energy Laboratory and Sandia National Laboratories provided guidance with regard to Extreme Condition Modeling which formed the basis of the methodology utilized in this project.

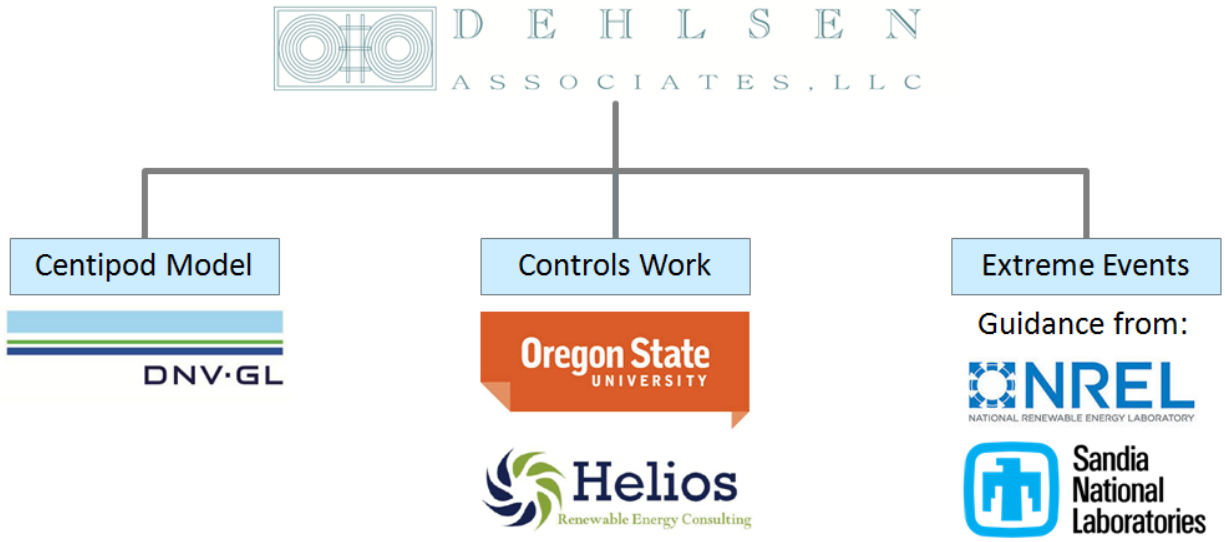

5.0 Project Task Activities

5.1 Task 1.0 - Develop reduced model representation for Centipod

The objective of Task 1 was to produce a reduced order model of Centipod, created in MATLAB, and verified against the more complex WaveDyn model. This reduced order model served two purposes. First, it was a fast and sufficiently accurate plant model to provide closed loop feedback during the development of the controller in MATLAB. Without the plant model, the controller would have had to be developed and run in C-code with WaveDyn providing closed loop feedback. This would have made both the development and simulation orders of magnitude slower.

In addition to representing the Centipod for closed loop feedback, the plant model is also an integral part of the fundamental operation of this specific estimation and control strategy. The plant model is used in the estimator (to estimate the excitation force acting on the body using only measured signals of position, velocity, and Fpto) and it is "model" portion of model predictive control (used to optimize the control action based on the expected plant response).The development of this model started with the general basis shown below:

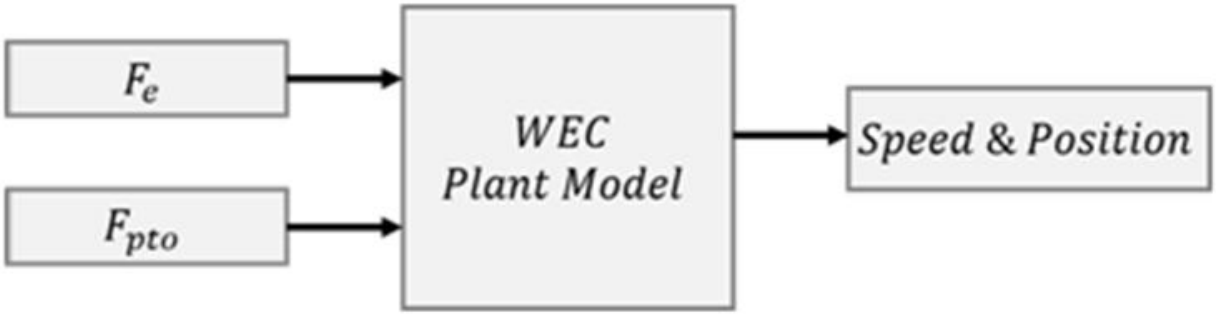

Figure 5.1.1: Basis of Centipod plant model.

The plant model is a state-space representation of the pod which is used to calculate and track position and velocity as well as several additional, unobservable states. This is a key component used by the MPC controller in that it is the model on top of which predictive control is executed. A simplified, frequency independent version of the plant model is given as:

$$\frac{d}{dt}\begin{bmatrix}\dot{z}\\ z\end{bmatrix} = \underbrace{\begin{bmatrix}\frac{-B}{m+A} & \frac{-k}{m+A}\\ 1 & 0\end{bmatrix}}_{A}\begin{bmatrix}\dot{z}\\ z\end{bmatrix} + \underbrace{\begin{bmatrix}\frac{1}{m+A}\\ 0\end{bmatrix}}_{Bu}\begin{bmatrix}F_{pto}\end{bmatrix} + \underbrace{\begin{bmatrix}\frac{1}{m+A}\\ 0\end{bmatrix}}_{Bv}\begin{bmatrix}F_e\end{bmatrix}$$

Where:

z	–	Pod/PTO position
z dot	–	Pod/PTO velocity
B	–	Hydrodynamic damping
A	–	Hydrodynamic added mass
m	–	Pod mass
k	–	Hydrodynamic stiffness
Fe	–	Hydrodynamic excitation force
Fpto	–	PTO force

The added mass and damping components (*A* and *B*) of the above formula are body geometry and mass derived outputs from a boundary element method (BEM) solver such as WAMIT. In reality, these values are also frequency dependent, meaning they differ depending on the wave frequency, which is variable throughout any real time series. A plot illustrating this frequency dependence is shown below:

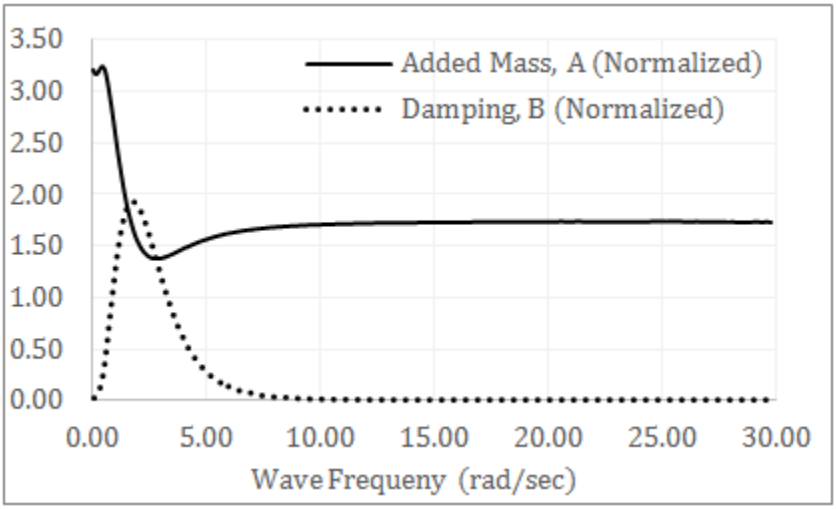

Figure 5.1.2: Normalized added mass and damping vs. wave frequency for an example WEC modelled in a BEM solver [1].

Since real sea conditions are not of uniform wave frequency, it was critical that the frequency dependent added mass and damping parameters be incorporated into the model rather than frequency independent values. This is well illustrated in the comparison of the two methods

against WaveDyn, a commercially available wave energy converter dynamics software package which has been experimentally validated, and thus serves as the source of truth in these figures.

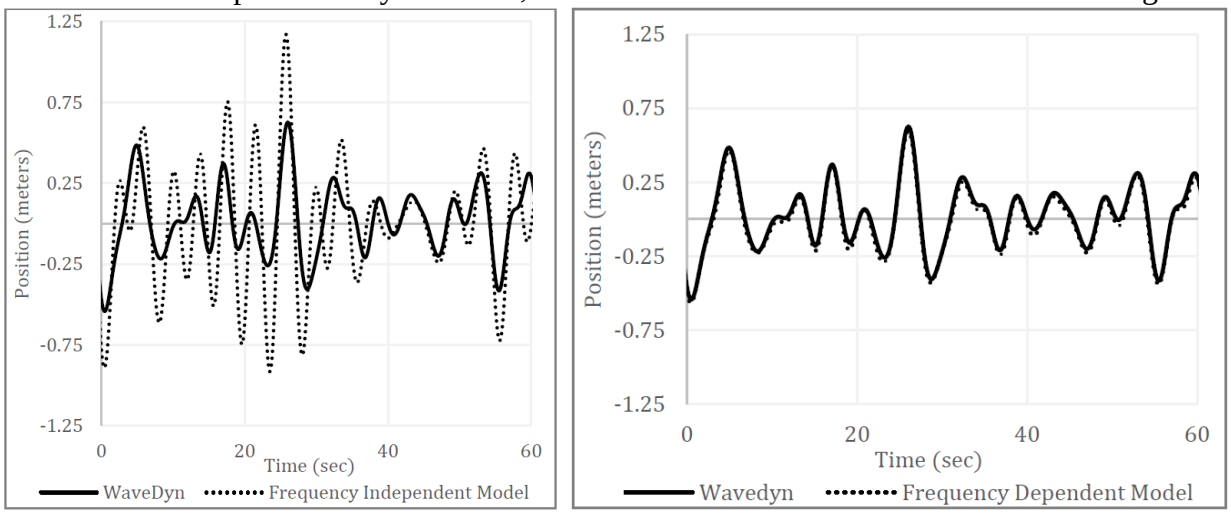

Figure 5.1.3: Comparison of Frequency Independent and Dependant models.

With the completion of a plant model for a single pod, the single pod plant model was extended to a multi-pod model which represented the complete Centipod WEC structure. The initial implementation of the full five pod system did not incorporate pod-to-pod interactions which would exist in a multiple pods placed in proximity to each other. This cross-coupling force is manifested through a body-to-body radiative force, *Fr*, and can be understood as waves created by the motion of one body acting as an external force on another body. To examine the importance of including this body-to-body interaction, the five pod model as augmented to include frequency dependent cross-coupling and the relative magnitudes of each force were compared. As is shown in Figure 5.1.5 for Pod 3, the external excitation force is significantly larger than all radiative forces, and the self-radiation force (Fr33) is furthermore much larger than cross-terms which are almost indiscernible along the x-axis.

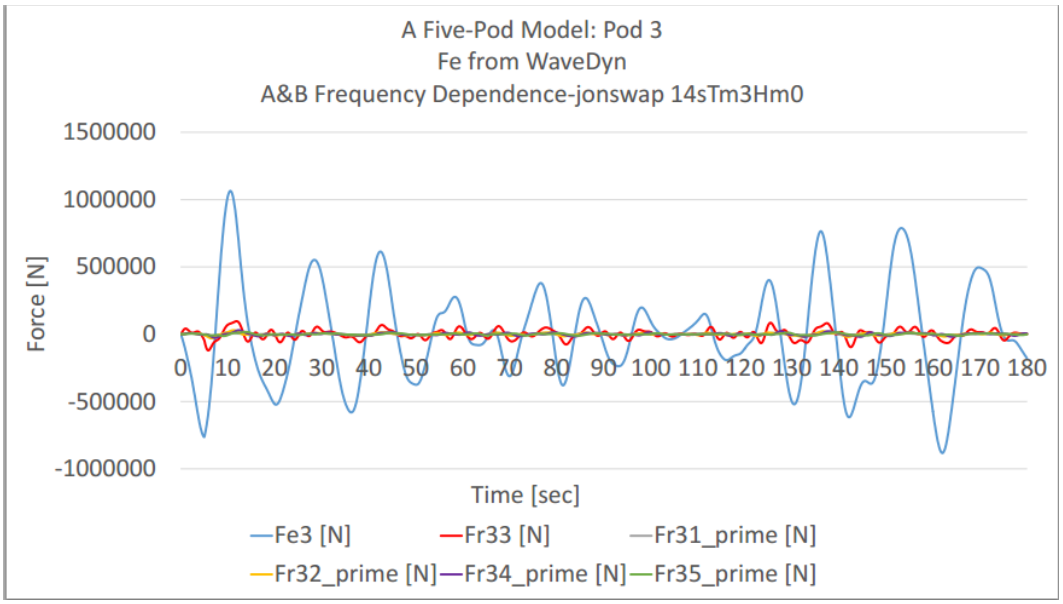

Figure 5.1.4: Excitation force of Pod 3 (blue) vs. all other pods radiation forces on Pod 3.

Given that the controller is being developed to run in real time, the team decided to omit the cross-coupling forces on the basis of their small relative magnitude. The five body plant model without cross-coupling was then validated against WaveDyn and confirmed to be accurate.

5.2 Task 2.0 - Develop baseline global integration model in WaveDyn

The numerical model of Centipod was created in DNV GL's WaveDyn software with the assistance of DNV GL. The construction of the numerical model was comprised of two parts: calculation of hydrodynamic data, and creation of the model itself within WaveDyn.

In order to obtain the hydrodynamic data for Centipod's geometry, a mesh of the WEC's wetted geometry was created from the existing CAD files. This mesh was then fed into WAMIT, a BEM hydrodynamics solver, alongside parametric data describing each of the 6 bodies of the WEC. WAMIT was then used to compute the hydrodynamic data, which would be fed into WaveDyn.

5.2.1 Hydrodynamics Data

The hydrodynamic coefficients and the wave exciting force associated with each body and the interactions between them were loaded into the 'Hydrodynamics' model from WAMIT. The hydrodynamics data were limited to first-order (linear) quantities. The model geometry used by the flow solver was defined using the Rhinoceros 3D modeling tool. This allows the definition of the geometry to be represented as splines for use with the high-order method option in WAMIT. An example of the mean wetted profile of the Centipod WEC is shown in Figure 5.2.1 and Figure 5.2.2. The mesh and frequency resolution were refined to allow the accurate representation of specific hydrodynamic quantities such as the radiation force.

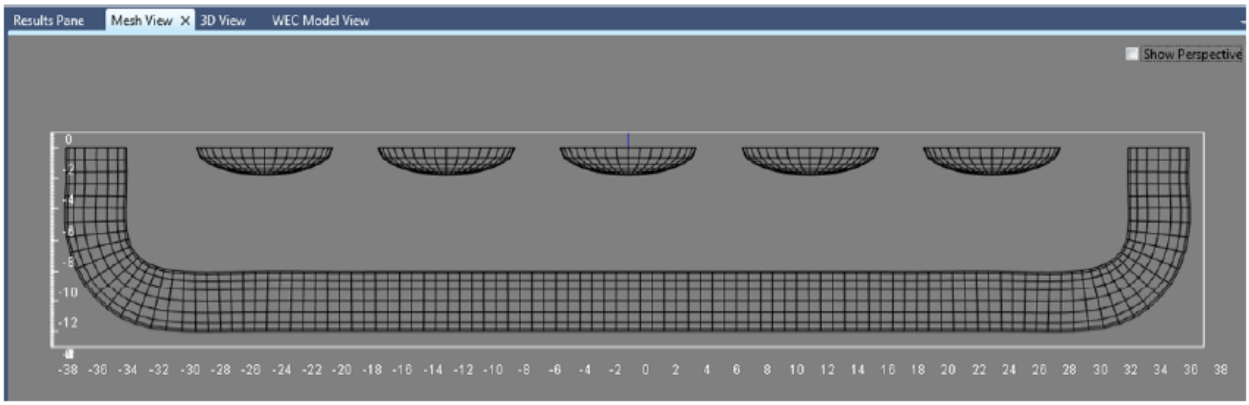

Figure 5.2.1: Profile showing the WAMIT mesh for a maximum panel size of 0.8m

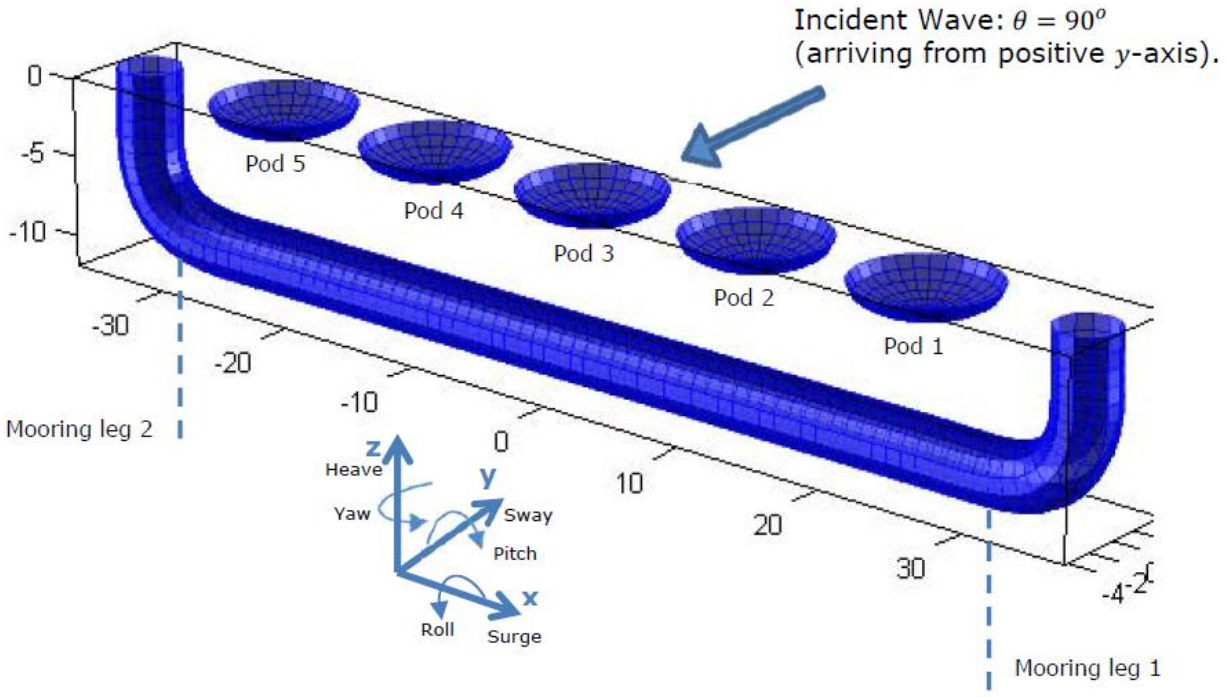

Figure 5.2.2: 3D view showing coordinate system of Centipod within WaveDyn.

The final set of hydrodynamic data was derived following a convergence exercise focusing on the mesh resolution. Convergence studies have investigated the frequency resolution, radiation damping decay at high and low frequencies and length of impulse response functions. The following describes the convergence study methodology DNV GL used focusing on the mesh resolution.
The mesh resolution of the pods was checked for convergence with special focus on the heave excitation force and radiation damping. The hydrodynamic data presented in this section for Pod 3 includes the influence of the 'backbone' and other pods in the vicinity. The focus for the excitation force convergence was on frequencies below 6rad/s, around 1s period, since for the sea-states investigated the energy beyond this frequency is negligible. The radiation damping was checked for convergence over a wider frequency range, providing a high level of confidence in values up to the frequencies where damping converged to zero (the complete set of data is integrated over all frequencies by the WaveDyn pre-processor). The WAMIT highorder method was used to discretize the wetted surface of the bodies and WAMIT was provided with a nominal 'Panel Size' characteristic length as a means of controlling the overall geometric resolution. For this investigation, the values used for the panel size parameter were 2m, 1m and 0.8m.

Figure 5.2.3 and Figure 5.2.5 show that the excitation amplitudes for the pods have converged for every mesh size up until around 2.5rad/s. For higher frequencies the 2m mesh appears to be of insufficient resolution. A mesh of 1m is sufficient for convergence up until around 6rad/s.

The radiation damping in heave also requires the panel size to be 1m before convergence is seen and it decays to zero within the frequency range considered, as shown in Figure 5.2.4. However

in sway (for translational motions in *y* – please see the axis orientations in Figure 5.2.2), the radiation damping (illustrated in Figure 5.2.6) only approaches zero for the highest frequencies studied. The non-complete decay to zero in the radiation damping is expected to have a very small effect on the final impulse response functions. Also a mesh size of 0.8m appears marginally superior in this case.

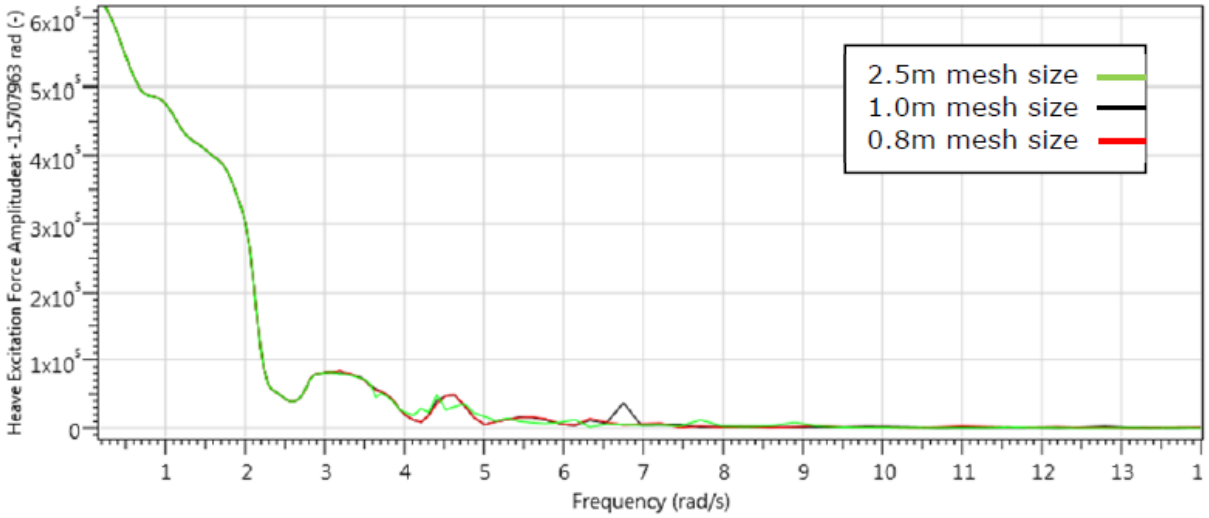

Figure 5.2.3: Heave excitation amplitude of Pod 3 for various mesh sizes with waves approaching from the positive global y axis.

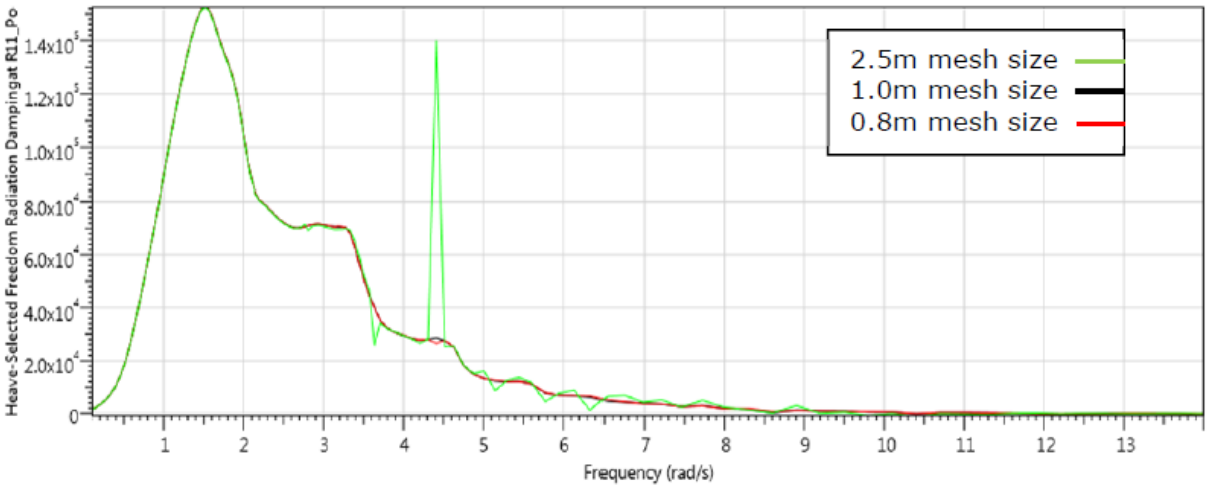

Figure 5.2.4: Heave radiation damping of Pod 3 for various mesh sizes.

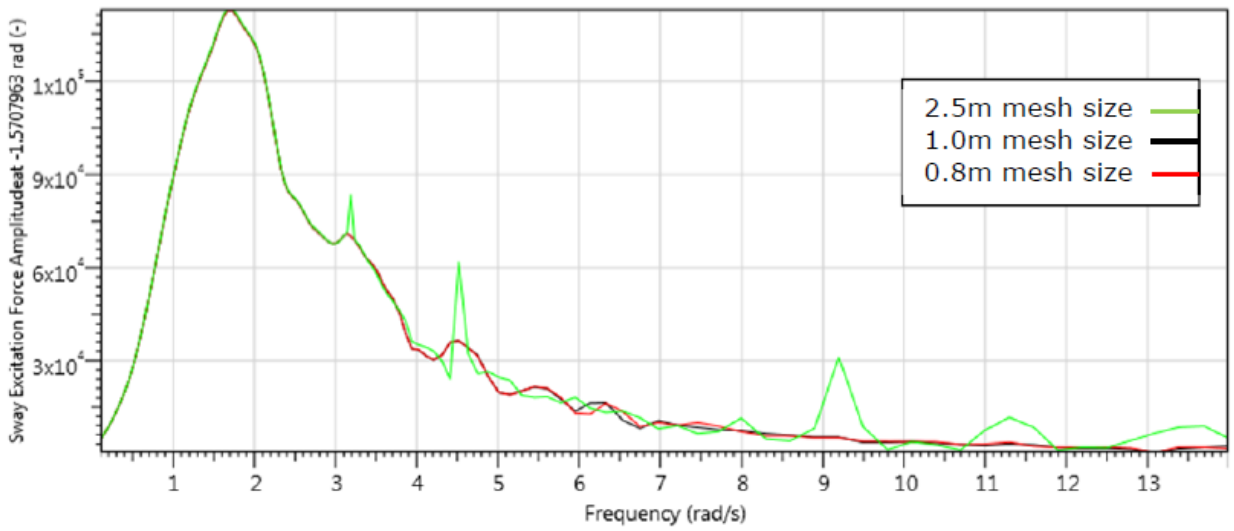

Figure 5.2.5: Sway excitation amplitude of Pod 3 for various mesh sizes with waves approaching from the positive global y axis.

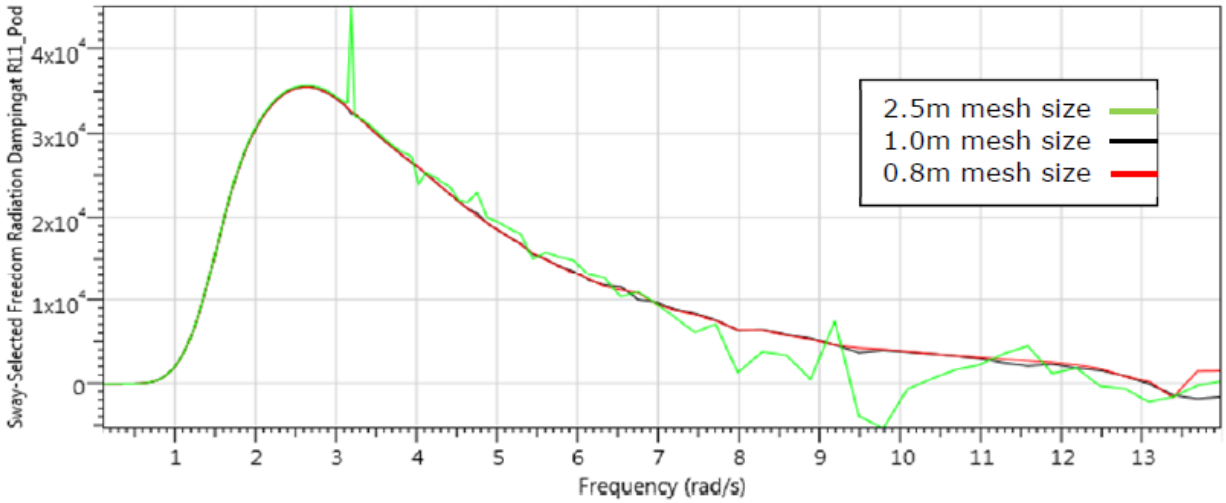

Figure 5.2.6: Sway radiation damping of Pod 3 for various mesh sizes.

5.2.2 WaveDyn Model

The WEC structural properties are represented in WaveDyn as rigid bodies with mass, moments of inertia and hydrodynamic properties. The component connectivity is defined using a series of nodes and massless rigid links which represent the physical offsets between individual parts of the WEC system. A block diagram representing the multi-body structure implemented in WaveDyn is provided in Figure 5.2.9.

A ground node, placed at the ‘backbone’ proximal node (0,0,60m), is connected via a floating free joint to the ‘backbone’ structure node, allowing it to float unrestrained in all 6 degrees-of freedom. The ‘Pod Attachment’ links provide the necessary horizontal offsets along the ‘backbone’ to the PTO units directly below each pod. A sliding joint PTO is used between the ‘backbone’ and each pod allowing single degree of freedom motion in the heave direction. A

rigid connection links each sliding joint to the center of mass of the corresponding pod. At the connection point between each pod's corresponding sliding PTO joint and the 'backbone' an additional hinge joint provides a further degree of freedom for rotational motion of the PTO and pod about the 'backbone' in the primary wave direction. This compliance is expected to reduce large moment arms which otherwise could have been experienced at the structural joint.

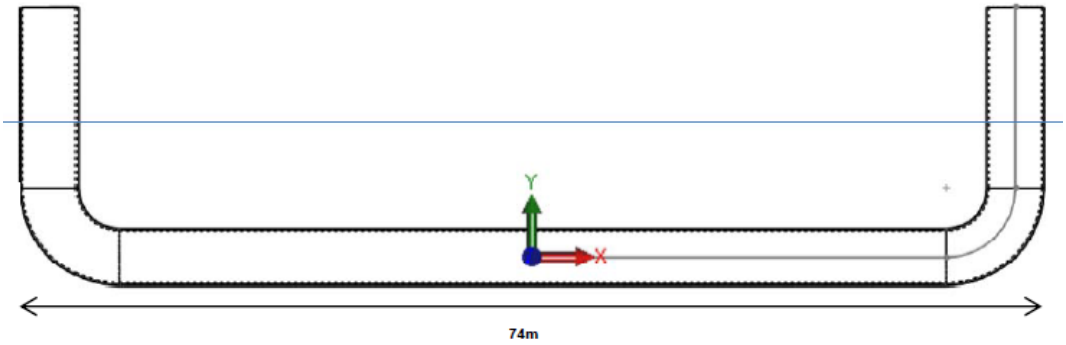

Figure 5.2.7: Reference coordinate system used by DA of 'backbone' center of gravity in Table 5.2.3. (Note that WaveDyn uses a coordinate system where the z-axis is vertical)

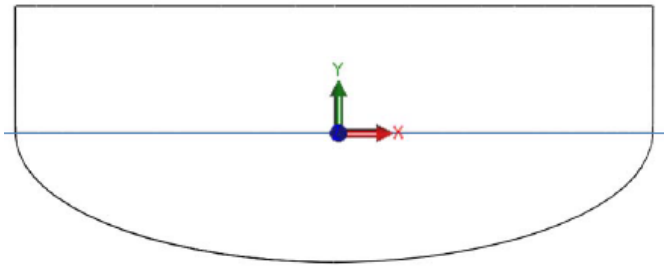

Figure 5.2.8: Reference coordinate system used by DA of pod center of gravity in Table 5.2.3. (Note that WaveDyn uses a coordinate system where the z-axis is vertical). The center of mass is located at the center of the body at the waterline. Not shown to scale with Figure 5.2.7.

The completed block diagram of Centipod modeled in WaveDyn can be seen below in Figure 5.2.9.

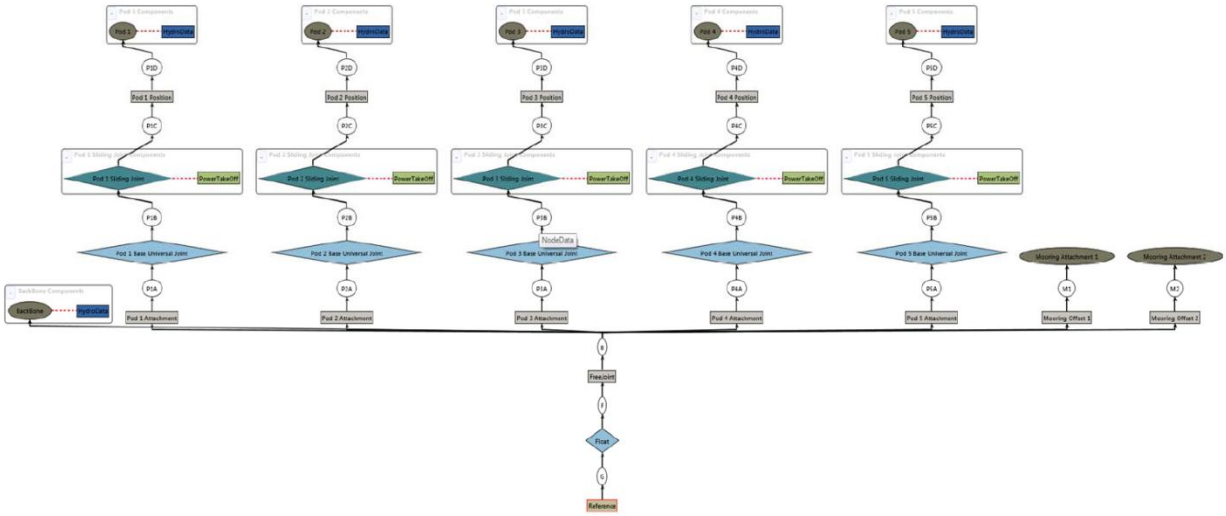

Figure 5.2.9: WaveDyn block diagram of Centipod.

5.3 Task 3.0 - Baseline performance and operational loads calculations

5.3.1 Performance Calculation:

5.3.1.1 Baseline Controller:

The baseline power take off (PTO) control scheme is fixed passive damping. This method applies a single damping value to the power take off system across all sea states. In order to optimize the damping value, the pod geometry and joint probability distribution (JPD) of the reference site both need to be considered. The optimal damping value is found using the formula below [3].

$$B_m = B_{m\,opt} = \left(B_r{}^2 + \left(\omega(m_m + m_r) - \frac{(\rho_w g S_w)}{\omega} \right)^2 \right)^{1/2}$$

Where:

B_m	–	PTO Damping Coefficient (Ns m^{-1})
B_r	–	Added Damping Coefficient (or 'Radiation Resistance') (Ns m^{-1})
$B_{m\,opt}$	–	Optimum PTO damping rate for maximum energy absorption (Ns m^{-1})
m_m	–	Physical mass (kg)
m_r	–	Added mass (kg)
S_w	–	Water plane area(m^2)
Ω	–	Wave frequency (rad s^{-1})

This calculation was conducted using a wave frequency matching the most probable portion of the reference site JPD and the added mass from the WAMIT output data set at that wave period. The optimal PTO damping coefficient resulting from this work was 688 kNs m^{-1}.

5.3.1.2 Power Matrix Methodology:

Using the model created as part of Task 2, DNV GL was able to run the WaveDyn model of Centipod for a number of different sea states representative of the resource supplied by DA. The resource supplied was that from the April 2013 *Standardized Cost and Performance Reporting for Marine and Hydrokinetic Technologies* paper [4] which outlined the DOE's preferred resource for use in LCOE calculations.

The performance data was generated as specified, creating a time series of length 200 times the peak period from a Bretschneider Spectrum with a peak period interval of one second. Each of the 190 sea states were run for 200 times the peak period with a ramp-up period of 5s. The first 10 seconds of simulation where not included in the mean power calculation to omit unrealistic initial settling motions, however it was assumed to have a minimal impact on total mean power.
The mean power over each bin's time series simulation was input into a mechanical power matrix and multiplied by the JPD, and other modifying factors to reach the final AEP estimation for the baseline.

5.3.1.3 AEP Calculation:

The AEP calculation method used the following procedure starting with the JPD and Mechanical Power Matrix:

Significant Wave Height, Hs [m] \ Peak Period, Tp [sec]	1.7	2.7	3.7	4.7	5.7	6.7	7.7	8.7	9.7	10.7	11.7	12.7	13.7	14.7	15.7	16.7	17.7	18.7	19.7	20.7
0.25	0.00%	0.00%	0.00%	0.00%	0.00%	0.01%	0.00%	0.00%	0.00%	0.00%	0.00%	0.00%	0.00%	0.01%	0.00%	0.00%	0.00%	0.00%	0.00%	0.00%
0.75	0.00%	0.00%	0.01%	0.15%	0.43%	1.07%	1.12%	1.30%	0.41%	0.63%	0.28%	0.20%	0.20%	0.34%	0.43%	0.48%	0.17%	0.00%	0.03%	0.00%
1.25	0.00%	0.00%	0.02%	0.10%	0.98%	2.80%	2.38%	4.56%	1.85%	2.16%	1.12%	0.87%	0.66%	0.55%	0.37%	0.44%	0.24%	0.00%	0.05%	0.00%
1.75	0.00%	0.00%	0.00%	0.03%	0.25%	2.47%	2.67%	3.64%	2.09%	3.53%	1.95%	1.36%	1.21%	0.95%	0.46%	0.51%	0.29%	0.00%	0.11%	0.00%
2.25	0.00%	0.00%	0.00%	0.00%	0.04%	0.64%	2.32%	3.56%	1.65%	3.27%	2.45%	1.86%	1.51%	1.03%	0.56%	0.51%	0.31%	0.00%	0.12%	0.00%
2.75	0.00%	0.00%	0.00%	0.00%	0.00%	0.19%	0.90%	2.73%	1.00%	2.16%	1.96%	1.51%	1.34%	0.85%	0.52%	0.49%	0.33%	0.00%	0.14%	0.00%
3.25	0.00%	0.00%	0.00%	0.00%	0.00%	0.03%	0.18%	1.06%	0.69%	1.21%	1.29%	1.19%	1.05%	0.83%	0.49%	0.43%	0.19%	0.00%	0.07%	0.00%
3.75	0.00%	0.00%	0.00%	0.00%	0.00%	0.00%	0.04%	0.29%	0.32%	0.53%	0.75%	0.68%	0.70%	0.60%	0.34%	0.27%	0.12%	0.00%	0.06%	0.00%
4.25	0.00%	0.00%	0.00%	0.00%	0.00%	0.00%	0.00%	0.09%	0.10%	0.18%	0.28%	0.34%	0.41%	0.36%	0.22%	0.23%	0.09%	0.00%	0.03%	0.00%
4.75	0.00%	0.00%	0.00%	0.00%	0.00%	0.00%	0.00%	0.01%	0.03%	0.07%	0.08%	0.12%	0.18%	0.24%	0.15%	0.16%	0.07%	0.00%	0.03%	0.00%
5.25	0.00%	0.00%	0.00%	0.00%	0.00%	0.00%	0.00%	0.00%	0.01%	0.01%	0.03%	0.05%	0.09%	0.12%	0.09%	0.10%	0.05%	0.00%	0.02%	0.00%
5.75	0.00%	0.00%	0.00%	0.00%	0.00%	0.00%	0.00%	0.00%	0.00%	0.00%	0.00%	0.01%	0.03%	0.05%	0.04%	0.05%	0.02%	0.00%	0.01%	0.00%
6.25	0.00%	0.00%	0.00%	0.00%	0.00%	0.00%	0.00%	0.00%	0.00%	0.00%	0.00%	0.01%	0.01%	0.04%	0.02%	0.03%	0.02%	0.00%	0.00%	0.00%
6.75	0.00%	0.00%	0.00%	0.00%	0.00%	0.00%	0.00%	0.00%	0.00%	0.00%	0.00%	0.00%	0.01%	0.01%	0.01%	0.01%	0.01%	0.00%	0.00%	0.00%
7.25	0.00%	0.00%	0.00%	0.00%	0.00%	0.00%	0.00%	0.00%	0.00%	0.00%	0.00%	0.00%	0.00%	0.00%	0.01%	0.01%	0.00%	0.00%	0.00%	0.00%
7.75	0.00%	0.00%	0.00%	0.00%	0.00%	0.00%	0.00%	0.00%	0.00%	0.00%	0.00%	0.00%	0.00%	0.00%	0.00%	0.00%	0.00%	0.00%	0.00%	0.00%
8.25	0.00%	0.00%	0.00%	0.00%	0.00%	0.00%	0.00%	0.00%	0.00%	0.00%	0.00%	0.00%	0.00%	0.00%	0.00%	0.00%	0.00%	0.00%	0.00%	0.00%
8.75	0.00%	0.00%	0.00%	0.00%	0.00%	0.00%	0.00%	0.00%	0.00%	0.00%	0.00%	0.00%	0.00%	0.00%	0.00%	0.00%	0.00%	0.00%	0.00%	0.00%

Figure 5.3.1: Northern California Joint Probability Distribution [4].

The mechanical power matrix was then modified to account for a uniformly applied 85% efficiency, a rated power of 1500kW and a cut off sea state of 5m Hs and greater. Per AEP calculation guidance [4] a 10% array loss and 95% availability were then applied. The resulting baseline AEP was then used to show relative improvement with MPC, as can be seen in Section 5.5.

5.3.2 Operational Loads:

5.3.2.1 Operational Loads Methodology:

The loads on the various WEC components are calculated (and output) within WaveDyn for all the elements in the structure. For the Centipod machine, the loads on the pods, mooring loads and loads on the PTO are considered the outputs of most interest. A statistical analysis of the loads has been performed (min, max, mean, standard deviation). The non-exceedance curves for the various sea states have also been calculated. The use of this type of output allows a good understanding of the various loads levels experienced by the WEC components. It also provides a useful way to compare the influence on the loads of changing the WEC configurations. The use of these cumulative probability curves can also be used at a later stage for loads extrapolation and fatigue analysis.

5.3.2.1 Operational Loads Results:

Loads were analyzed and post processed for a number of nodes on the Centipod device under baseline operational conditions. The most critical to the structural design, and the load directly influenced by controller choice, is the axial force at each Pod connection. An identical methodology was utilized for the analysis of loads after implementation of MPC, this will be further described in Section 5.5.

5.4 Task 4.0 - Develop model predictive control framework

5.4.1 Controller overview:

The MPC controller developed in this work is a state-space, "look ahead" controller approach using knowledge of past and current states to predict future states to take action with the PTO to maximize power capture while still respecting system constraints. In order to maximize power, which is the productof force and velocity, the controller must aim to create phase alignment between excitation force and velocity.

A diagram of the developed controller is shown below in Figure 5.4.1.

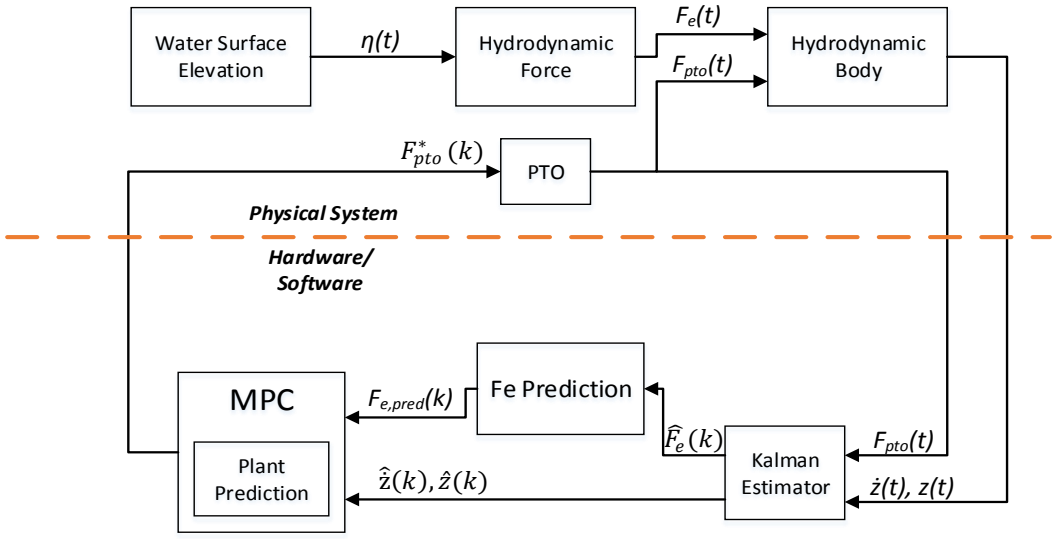

Figure 5.4.1: Controller block diagram

The controller has a single output, PTO force (Fpto), and three inputs: Fpto, Pod position (z), and velocity ($\dot{z}$). This controller requires no external or up-stream measurement of waves, it simply makes use of the aforementioned PTO force, position, and velocity time series, inputs which can be obtained easily without additional sensors. These inputs are fed into an estimator that outputs the hydrodynamic excitation force (Fe) imparted on the pod along with several internal states. A prediction block is utilized to take this excitation force history and predict future excitation force through the horizon for control. The controller uses the estimated current state and the prediction of future excitation forces to find an optimal Fpto which maximizes power as the product of force and velocity.

The blocks within the controller are described in detail in the following sub-sections.

5.4.2 Kalman Estimator:

The estimator uses the known commanded Fpto, alongside the measured inputs for position and velocity to estimate the excitation force time series history. All other signals, including all plant states (measureable or otherwise) as well as the excitation force acting on each body, are estimated through a linear Kalman filter.

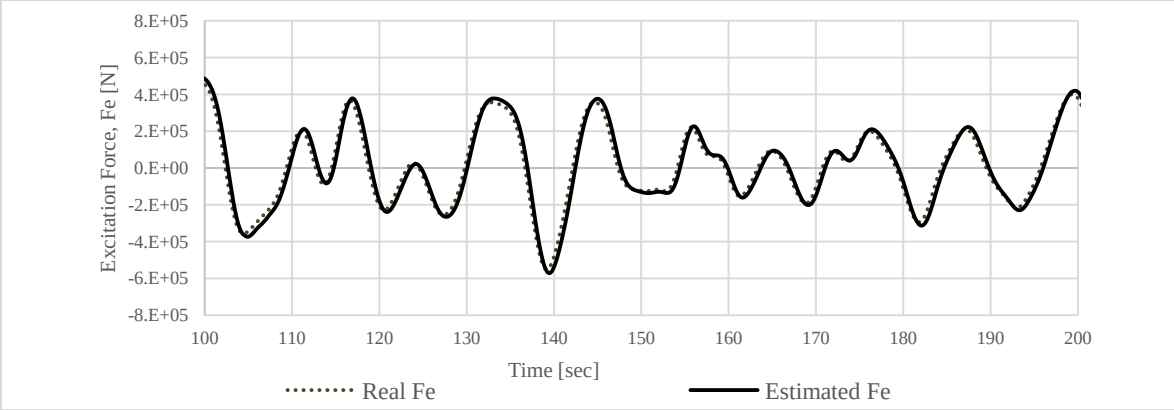

Figure 5.4.2: Estimate of excitation force, Fe, in a realistic sea state from Kalman filter using only measured velocity and position and the commanded PTO force [1].

In addition to that which is shown in the figure above, a strong correlation between the real and estimated excitation force was demonstrated across multiple sea states.

5.4.3 Fe Prediction:

Using previous and current estimated excitation force, an auto-regressive sliding window adaptive least-squares approach was used to model and predict future values. The output, future Fe prediction, is used as an input in the MPC block to inform Fpto selection. Where k is the current time and $k+H_p$ is the time horizon, the vector $F_e(k) \ldots F_e(k+H_p)$ can be calculated for each of the N total bodies in the WEC system at every time k through N independent iterations of the following [2]:

$$F_e(k+1|k) = \alpha_1 F_e(k) + \alpha_2 F_e(k-1) + \cdots + \alpha_n F_e(k-n+1) \quad (1)$$

$$F_e(k+2|k) = \alpha_1 F_e(k+1|k) + \alpha_2 F_e(k) + \cdots + \alpha_n F_e(k-n+2) \quad (2)$$

up to:

$$F_e(k+H_p|k) = \alpha_1 F_e(k+H_p-1|k) + \alpha_2 F_e(k+H_p-2|k) + \cdots + \alpha_n F_e(k+H_p-n|k) \quad (3)$$

$\alpha 1 \ldots \alpha n$ are calculated for each time in the observation horizon using a linear regression matrix [2]:

$$\begin{bmatrix} F_{e,k} \\ F_{e,k-1} \\ \vdots \\ F_{e,k-h} \end{bmatrix} = \begin{bmatrix} F_{e,k-1} & \cdots & F_{e,k-n} \\ F_{e,k-2} & \cdots & F_{e,k-1-n} \\ \vdots & \ddots & \vdots \\ F_{e,k-h-1} & \cdots & F_{e,k-h-n} \end{bmatrix} \begin{bmatrix} \alpha_1 \\ \vdots \\ \alpha_n \end{bmatrix} \quad (4)$$

The accuracy of Fe predicted in this way is only somewhat accurate and is more useful to consider as showing the overall expected trend of the excitation force over the prediction horizon.

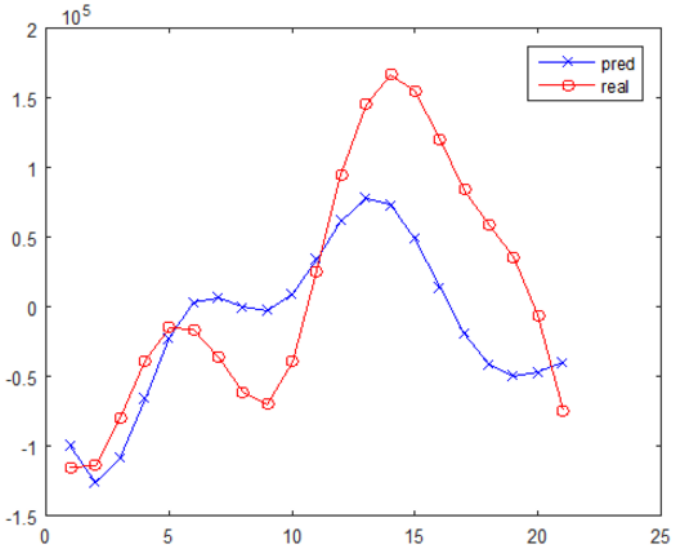

Figure 5.4.3: An example plot of real versus predicted Fe

Importantly, though, because MPC works on a wave-to-wave time scale to optimize power, the accuracy of this prediction strategy was determined to be sufficient by comparing power production using predicted values *vs.* known "test" future data. These results demonstrated less than 5% reduction in power production improvement when using predicted values from estimated excitation forces. In other, slower control schemes (*i.e.* slow active damping tuning) the prediction accuracy would likely be more important.

Various prediction horizons (Hp) were also investigated. Short prediction horizons would give an incomplete picture to the controller for optimizing power over the time horizon, while long time horizons would force the controller to optimize power using less accurate predictions of Fe far in the future. A balance between these two challenges was sought. Mean power was calculated on a number of time series from different sea states along with using the known future excitation force. This work led to the conclusion that a 10 second prediction horizon would yield the best performance. One example time series result is shown below in Figure 5.4.4.

	Hp	Estimated v_arrow_k in hessian and constraint	Real v_arrow_k in hessian and constraint
Power from Matlab	3	4.73E+04	5.29E+04
Infeasibility		5	1
Over max		0	0
	5	8.87E+04	9.72E+04
		7	1
		15	13
	8	1.06E+05	1.19E+05
		11	1
		17	18
	10	1.07E+05	1.20E+05
		14	1
		17	18
	15	1.06E+05	1.17E+05
		14	1
		14	21

Figure 5.4.4: Example mean power with varying prediction horizons, estimated Fe vs. real Fe

5.4.4 MPC:

The cornerstone of the MPC controller developed in this work is an optimization function which maximizes power as the product of force and velocity. The general form of the quadratic optimization function which achieves this outcome can be written as [2]:

$$\min J(x) = \frac{1}{2}x^T Hx + f^T x \tag{5}$$

Subject to

$$Ax \leq B \tag{6}$$

(5) can be re-written in terms specific to the MPC controller as shown below in (7)[2]:

$$J(k) = \frac{1}{2}\vec{\boldsymbol{y}}(k)^T \boldsymbol{Q}\vec{\boldsymbol{y}}(k) + \frac{1}{2}\vec{\boldsymbol{u}}(k)^T \boldsymbol{R}\vec{\boldsymbol{u}}(k) \tag{7}$$

$\vec{y}(k)$ represents states from the WEC from the current time, k, to the horizon, $k + H_p$, as given by the predictive plant model. Importantly, $\vec{y}(k)$ includes terms for both force and velocity which the matrix Q selects to multiply as power. The vector $\vec{u}(k)$ represents the rate of change in the force of the PTO (*i.e.* $\dot{F}_{pto}$) and serves as the control input for optimization. The matrix R penalizes controller action to reduce large swings in force. The result is that the minimization of $J(k)$ yields the control action $\dot{F}_{pto}$ (given in the vector $\vec{u}(k)$) which each WEC should apply at each step through the horizon to maximize power. As is typical to MPC, only $\dot{F}_{pto}$ for the current time is applied, and the controller re-runs at the next time step to repeat this process [2].

5.4.5 Constraints:

The constraints utilized for this work are considered hard constraints. The solver must find a solution which is within the bounds of all the constraints or else the solution is infeasible. In the event that the solution is infeasible, the most recent solution to satisfy the constraints is used. In future work alternate constraint methodologies will be explored to improve performance of the controller and reduce infeasibilities.

Due to the desire to model the benefit of MPC without being restricted by PTO choice, loose constraints were applied to create what is effectively an unconstrained controller for most operational seas. The constraints are as follows:

Fpto max	=	1000kN
Max PTO Stroke	=	effectively unconstrained – See Figure 5.5.3
Max PTO Velocity	=	+-3m/s

Further detail on the mathematics behind the MPC formulation can be found in [2] “Increasing Power Capture From Multibody Wave Energy Conversion Systems Using Model Predictive Control”.

5.5 Task 5.0 - MPC performance and operational loads calculation

5.5.1 Performance Calculation:

5.5.1.1 Implementation of MPC:

In order to incorporate the MPC controller into WaveDyn, the controller had to be re-written in C before it was linked with WaveDyn. To better utilize the framework developed in MATLAB, Armadillo, a high quality C++ linear algebra library, was used. Armadillo is aimed towards a good balance between speed and ease of use and the syntax (API) is deliberately similar to MATLAB. It is an open source library that can be used for both R&D and production environments. The convex optimization problem is solved using C code generated using qpOASES. This model provided a quick and efficient way to use the MATLAB code developed for MPC implementation.

With the controller re-written in C, the process of coupling the controller with WaveDyn began. Using the controller produced in C, a DLL was created to be run alongside WaveDyn as an external controller. This controller DLL also uses a number of separate input files, which contain all the physical constraints such as maximum stroke, velocity and force of the PTO. Since these input files are external to the DLL, the constraints can easily be modified without the need to re-compile the DLL, leading to a much easier environment for troubleshooting.
The impact of the utilization of MPC with the WEC was then evaluated through the creation of a power matrix.

5.5.1.2 Power Matrix Methodology:

Using the model created as part of Task 2, coupled with the controller, DNV GL was able to run the WaveDyn model of Centipod for a number of different sea states representative of the same reference resource used in the baseline assessment. The resource supplied was that from the April 2013 *Standardized Cost and Performance Reporting for Marine and Hydrokinetic Technologies* paper [4].

The performance data was generated as specified, creating a time series of length 200 times the peak period from a Bretschneider Spectrum for each sea state bin in the JPD. Each of the 190 sea states were run for 200 times the peak period. The short duration of simulation time prior to controller start-up was not included in the mean power calculation.

The mean power over each bin’s time series simulation was input into a mechanical power matrix and multiplied by the JPD, and other modifying factors to reach the final AEP estimation for the baseline.

5.5.1.3 AEP Calculation:

The AEP calculation was calculated from the JPD and Mechanical Power Matrix:

Significant Wave Height, Hs [m] \ Peak Period, Tp [sec]	1.7	2.7	3.7	4.7	5.7	6.7	7.7	8.7	9.7	10.7	11.7	12.7	13.7	14.7	15.7	16.7	17.7	18.7	19.7	20.7
0.25	0.00%	0.00%	0.00%	0.00%	0.00%	0.01%	0.00%	0.00%	0.00%	0.00%	0.00%	0.00%	0.00%	0.01%	0.00%	0.00%	0.00%	0.00%	0.00%	0.00%
0.75	0.00%	0.00%	0.01%	0.15%	0.43%	1.07%	1.12%	1.30%	0.41%	0.63%	0.28%	0.20%	0.20%	0.34%	0.43%	0.48%	0.17%	0.00%	0.03%	0.00%
1.25	0.00%	0.00%	0.02%	0.10%	0.98%	2.80%	2.38%	4.56%	1.85%	2.16%	1.12%	0.87%	0.66%	0.55%	0.37%	0.44%	0.24%	0.00%	0.05%	0.00%
1.75	0.00%	0.00%	0.00%	0.03%	0.25%	2.47%	2.67%	3.64%	2.09%	3.53%	1.95%	1.36%	1.21%	0.95%	0.46%	0.51%	0.29%	0.00%	0.11%	0.00%
2.25	0.00%	0.00%	0.00%	0.00%	0.04%	0.64%	2.32%	3.56%	1.65%	3.27%	2.45%	1.86%	1.51%	1.03%	0.56%	0.51%	0.31%	0.00%	0.12%	0.00%
2.75	0.00%	0.00%	0.00%	0.00%	0.00%	0.19%	0.90%	2.73%	1.00%	2.16%	1.96%	1.51%	1.34%	0.85%	0.52%	0.49%	0.33%	0.00%	0.14%	0.00%
3.25	0.00%	0.00%	0.00%	0.00%	0.00%	0.03%	0.18%	1.06%	0.69%	1.21%	1.29%	1.19%	1.05%	0.83%	0.49%	0.43%	0.19%	0.00%	0.07%	0.00%
3.75	0.00%	0.00%	0.00%	0.00%	0.00%	0.00%	0.04%	0.29%	0.32%	0.53%	0.75%	0.68%	0.70%	0.60%	0.34%	0.27%	0.12%	0.00%	0.06%	0.00%
4.25	0.00%	0.00%	0.00%	0.00%	0.00%	0.00%	0.00%	0.09%	0.10%	0.18%	0.28%	0.34%	0.41%	0.36%	0.22%	0.23%	0.09%	0.00%	0.03%	0.00%
4.75	0.00%	0.00%	0.00%	0.00%	0.00%	0.00%	0.00%	0.01%	0.03%	0.07%	0.08%	0.12%	0.18%	0.24%	0.15%	0.16%	0.07%	0.00%	0.03%	0.00%
5.25	0.00%	0.00%	0.00%	0.00%	0.00%	0.00%	0.00%	0.00%	0.01%	0.01%	0.03%	0.05%	0.09%	0.12%	0.09%	0.10%	0.05%	0.00%	0.02%	0.00%
5.75	0.00%	0.00%	0.00%	0.00%	0.00%	0.00%	0.00%	0.00%	0.00%	0.00%	0.00%	0.01%	0.03%	0.05%	0.04%	0.05%	0.02%	0.00%	0.01%	0.00%
6.25	0.00%	0.00%	0.00%	0.00%	0.00%	0.00%	0.00%	0.00%	0.00%	0.00%	0.00%	0.01%	0.01%	0.04%	0.02%	0.03%	0.02%	0.00%	0.00%	0.00%
6.75	0.00%	0.00%	0.00%	0.00%	0.00%	0.00%	0.00%	0.00%	0.00%	0.00%	0.00%	0.00%	0.01%	0.01%	0.01%	0.01%	0.01%	0.00%	0.00%	0.00%
7.25	0.00%	0.00%	0.00%	0.00%	0.00%	0.00%	0.00%	0.00%	0.00%	0.00%	0.00%	0.00%	0.00%	0.00%	0.01%	0.01%	0.00%	0.00%	0.00%	0.00%
7.75	0.00%	0.00%	0.00%	0.00%	0.00%	0.00%	0.00%	0.00%	0.00%	0.00%	0.00%	0.00%	0.00%	0.00%	0.00%	0.00%	0.00%	0.00%	0.00%	0.00%
8.25	0.00%	0.00%	0.00%	0.00%	0.00%	0.00%	0.00%	0.00%	0.00%	0.00%	0.00%	0.00%	0.00%	0.00%	0.00%	0.00%	0.00%	0.00%	0.00%	0.00%
8.75	0.00%	0.00%	0.00%	0.00%	0.00%	0.00%	0.00%	0.00%	0.00%	0.00%	0.00%	0.00%	0.00%	0.00%	0.00%	0.00%	0.00%	0.00%	0.00%	0.00%

Figure 5.5.1: Northern California Joint Probability Distribution [4].

Wave State vs. Mechanical Power Extraction

Hm0 (m) \ Tp (sec)	3.7	4.7	5.7	6.7	7.7	8.7	9.7	10.7	11.7	12.7	13.7	14.7	15.7	16.7	17.7	18.7	19.7
0.25				71%	97%			200%	250%	327%	392%	429%	505%		570%		
0.75	45%	53%	73%	98%	126%	157%	194%	226%	282%	345%	405%	412%	445%	513%	601%		594%
1.25	48%	52%	94%	116%	144%	175%	196%	232%	249%	324%	312%	351%	358%	357%	322%		344%
1.75	47%	49%	87%	120%	143%	196%	170%	175%	156%	238%	230%	285%	201%	295%	256%		351%
2.25		50%	85%	133%	158%	173%	147%	158%	172%	187%	191%	204%	196%	227%	269%		330%
2.75			100%	147%	173%	173%	138%	135%	135%	175%	170%	204%	198%	203%	190%		225%
3.25			76%	136%	166%	158%	145%	113%	128%	117%	177%	148%	156%	186%	190%		222%
3.75				121%	175%	134%	118%	112%	113%	129%	151%	161%	156%	179%	198%		218%
4.25					158%	142%	101%	112%	124%	135%	154%	149%	154%	151%	155%		232%
4.75						136%	112%	106%	104%	125%	126%	127%	182%	174%	175%		209%

Figure 5.5.2: Mechanical Power Matrix relative to baseline.

The mechanical power matrix was then modified to account for a uniformly applied 85% efficiency, a rated power of 1500kW and a cut off sea state of 5m Hs and greater. Per AEP calculation guidance [4] a 10% array loss and 95% availability were then applied. These modifications were identical to those applied to the Baseline Mechanical Power Matrix.

A final AEP was reached for the MPC enabled WEC. A 161% improvement over baseline AEP (or 2.61 times larger than the baseline) was shown.

With respect to the unconstrained nature of the PTO constraints used for this performance evaluation, it should be shown that the PTO stroke maintained realistic throughout the simulation.

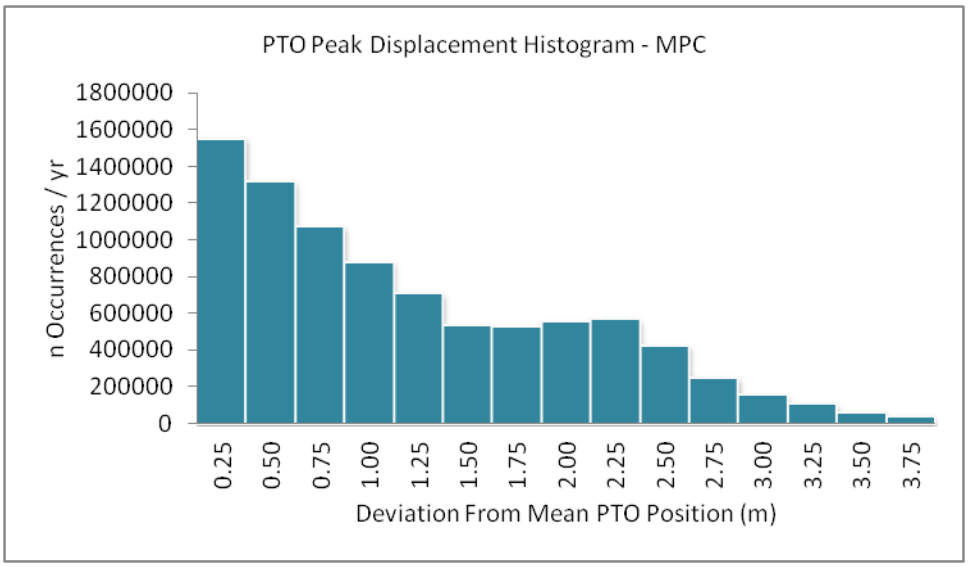

Figure 5.5.3: Peak PTO displacement histogram by occurrence annually.

The figure above demonstrates that, while unrestricted, the PTO stroke stayed within a reasonable bound. Furthermore, if a constraint were applied, the AEP would only be minimally affected.

5.5.2 Operational Loads:

5.5.2.1 Operational Loads Methodology:

Once again, for the comparative assessment of Centipod's loads with and without MPC, the loads on the various WEC components are calculated (and output) within WaveDyn for all the elements in the structure. For the Centipod machine, the loads on the pods, mooring loads and loads on the PTO are considered the outputs of most interest. A statistical analysis of the loads has been performed (min, max, mean, standard deviation). The non-exceedance curves for the various sea states have also been calculated. The use of this type of output allows a good understanding of the various loads levels experienced by the WEC components. It also provides a useful way to compare the influence on the loads of changing the WEC configurations. The use of these cumulative probability curves can also be used at a later stage for loads extrapolation and fatigue analysis.

5.5.2.2 Operational Loads Results:

Loads were analyzed and post processed for a number of nodes on the Centipod device under baseline operational conditions. The most critical to the structural design, and the load directly influenced by controller choice, is the axial force at each Pod connection. When compared to the baseline of maximum axial force, an increase in loads can be observed. Figure 5.5.4 shows the increase in maximum axial force, MPC relative to baseline.

Maximum Axial Force Increase (%)

Hm0 (m) \ Tp (sec)	3.7	4.7	5.7	6.7	7.7	8.7	9.7	10.7	11.7	12.7	13.7	14.7	15.7	16.7	17.7	18.7	19.7
0.25				248%	259%			435%	565%	712%	1041%	918%	944%		1236%		
0.75	73%	84%	132%	140%	169%	170%	300%	330%	423%	432%	431%	505%	401%	502%	504%		575%
1.25	76%	65%	67%	115%	125%	158%	283%	193%	280%	287%	256%	318%	279%	238%	275%		289%
1.75	49%	80%	49%	125%	130%	133%	157%	151%	172%	143%	173%	205%	196%	179%	187%		234%
2.25		48%	27%	53%	93%	74%	91%	97%	92%	142%	117%	77%	109%	143%	134%		171%
2.75			16%	36%	77%	90%	73%	55%	56%	86%	94%	101%	84%	75%	99%		124%
3.25			-10%	42%	49%	51%	53%	49%	36%	80%	41%	51%	93%	72%	81%		107%
3.75				28%	35%	39%	36%	54%	46%	55%	35%	50%	62%	59%	46%		81%
4.25					13%	19%	43%	18%	36%	38%	25%	65%	46%	41%	36%		60%
4.75						15%	22%	19%	7%	13%	-4%	21%	47%	31%	40%		17%

Figure 5.5.4: Relative maximum axial force for Pod 3 for all sea states investigated.

The most significant load increases occur primarily in small significant wave height sea states. This is tied to the MPC enabled system's capability of better extracting energy from smaller sea states, thus larger forces are observed. Critically, the maximum forces in the higher energy sea states only show minor increases in MPC relative to baseline. This, coupled with the knowledge that most of the ultimate loads will occur in extreme sea state conditions, rather than operational loads, lead to the conclusion that the implementation of MPC will not have a significant impact on any ultimate load driven structural requirements.

Cyclic loading and fatigue driven design requirements, however, will be significantly impacted by the implementation of MPC. The following, Figure 5.5.5, shows the annual loading histogram with MPC and baseline.

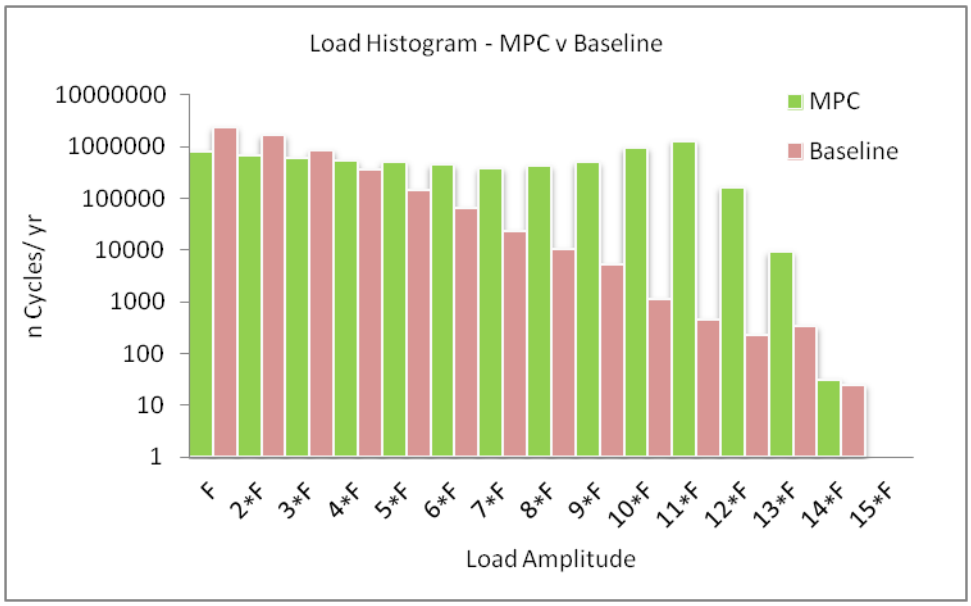

Figure 5.5.5: Load histogram by annual occurrences.

Figure 5.5.5 was produced by using the WAFO Toolbox for MATLAB [5] recording the peak force of each wave in each 200*Tp time series per sea state. All 190 sea states were multiplied by their occurrence probability in the JPD to reach an annual number of cycles for each load bin

shown in the histogram. This loading histogram was then used in the System Impact analysis, which will be further discussed in Section 5.7, to help identify the impact of MPC on structural requirements of Centipod.

5.6 Task 6.0 - Extreme sea state load calculations

5.6.1 Methodology:

A proper investigation into Extreme Conditions Modelling (ECM) requires identification of load cases through analysis various sea states and modes of operation in a mid-fidelity tool such as WaveDyn or WECSim, followed by a thorough study of these load cases with a high-fidelity (CFD) tool. This project does not allow for the full scope of a complete ECM study. Thus only the identification of load cases and relative loading between modes of operation will be completed in a mid-fidelity tool (WaveDyn). It is especially of interest how extreme loads of a baseline (fixed damping control) Centipod WEC compare to the same WEC employing 'detuned' MPC control. The results of this study will be adequate for roughly quantifying the relative loading of these techniques, but will fall short of what is needed to complete a structural design of the Centipod WEC.

The procedure for this study is broken down into five stages:

1) Identify the candidate sea states
2) Determine the number of seeds required
3) Investigate various wave headings (using baseline)
4) Identify the load cases of interest

Identify the candidate sea states: The site considered for all work undergone in this project was the DOE LCOE reference site in Northern California. This site's 100 year wave contour was published by Sandia National Labs in *Extreme Ocean Wave Conditions for Northern California Wave Energy Conversion Device* [6].

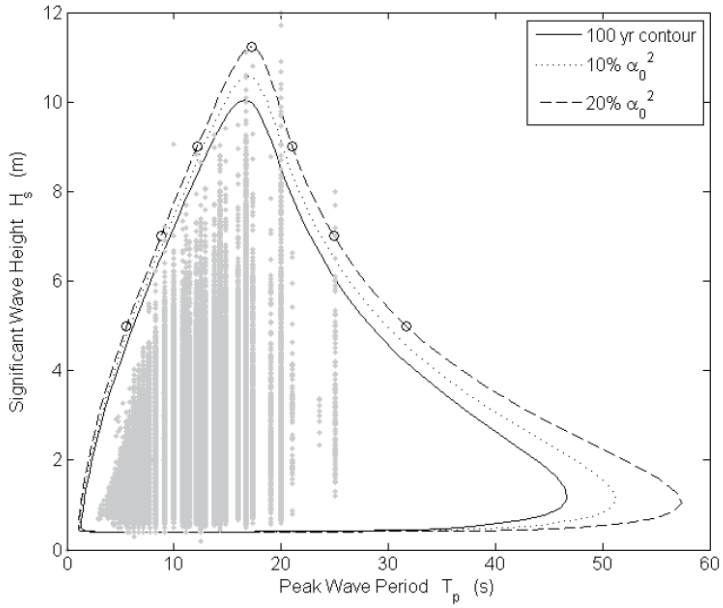

Significant wave height Hs (m)	5	7	9	11.22	9	7	5
Peak period Tp (s)	5.57	8.76	12.18	17.26	21.09	24.92	31.70

Figure 5.6.1: 100 yr. wave contour with candidate sea states [6].

Each of the sea states of interest along this contour was modelled with differing wave directions. The sea state and direction combinations yielding the highest loads were used for comparison with the MPC model variant.

Determine the number of seeds required: A convergence study was conducted to determine the number of seeds required for a good representation of each sea case. A seed is used to randomly generate a time series of wave elevation given significant wave height (Hs) and peak period (Tp). If the seed is the same, it will generate the same time series repeatedly, however each time series is created using a randomly generated seed and thus a random time series results. All the simulations used a time series duration of 200*Tp, thus the number of seeds required represents the number of randomly generated waves within a sea state required to converge upon a set of results.

A model was run through WaveDyn under a certain sea state (Hs, Tp, and direction) the results were then post-processed in MATLAB using the Wave Analysis for Fatigue and Oceanography (WAFO) toolbox [5] to identify each peak within the time series.

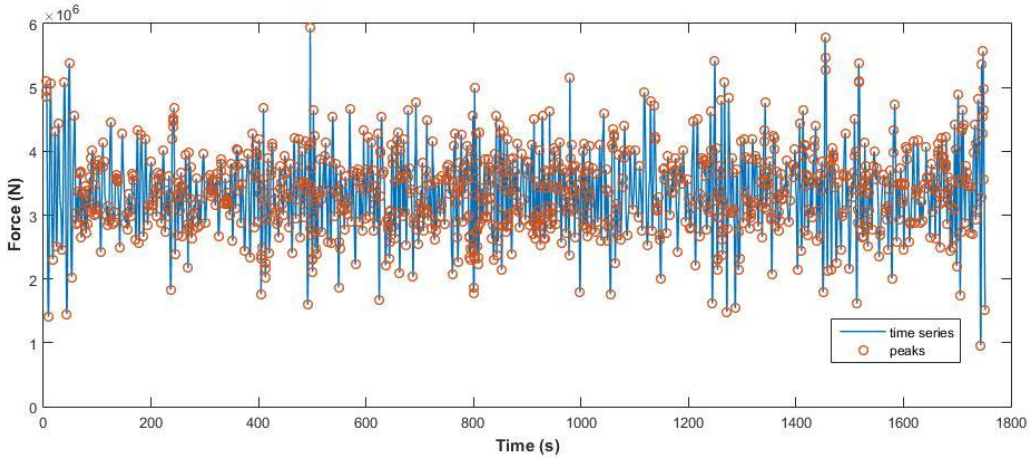

Figure 5.6.2: Peaks identified from time series.

The peaks were collected into a new vector within MATLAB. From the peaks vector, a non-exceedance plot was created to represent the probability of loads occurring for a given sea state.

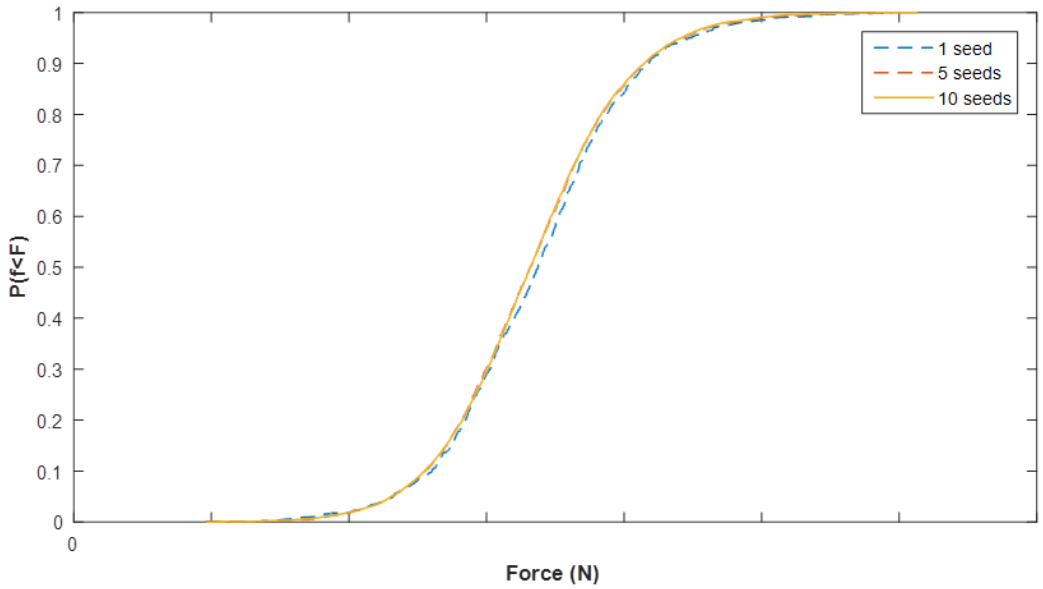

Figure 5.6.3: Non-exceedance plot of mooring tension for 1, 5, and 10 seeds.

From the results of this plot it can be seen that the load probability converges around 5 seeds, with any more seeds leading to a similar result.

Investigate various wave headings (using baseline): 0, 45, and 90 degree unidirectional waves were modelled at a given sea state. The coordinate system is shown along with the results of these three wave direction cases for some loads of interest.

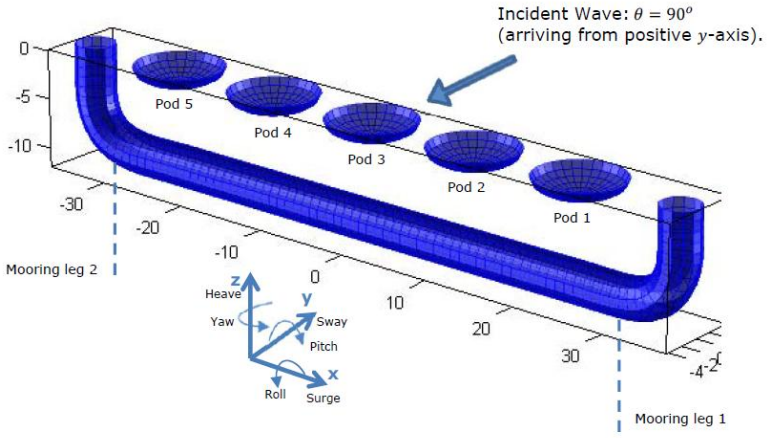

Figure 5.6.4: Coordinate system of Centipod.

The loads of interest in this investigation were:

1) Mooring line tension
2) PTO force in the heave direction (Pod 3 was used)
3) Pitch Moment at Pod Hinge connection (Pod 1 was used)

These loads are shown on the diagram below:

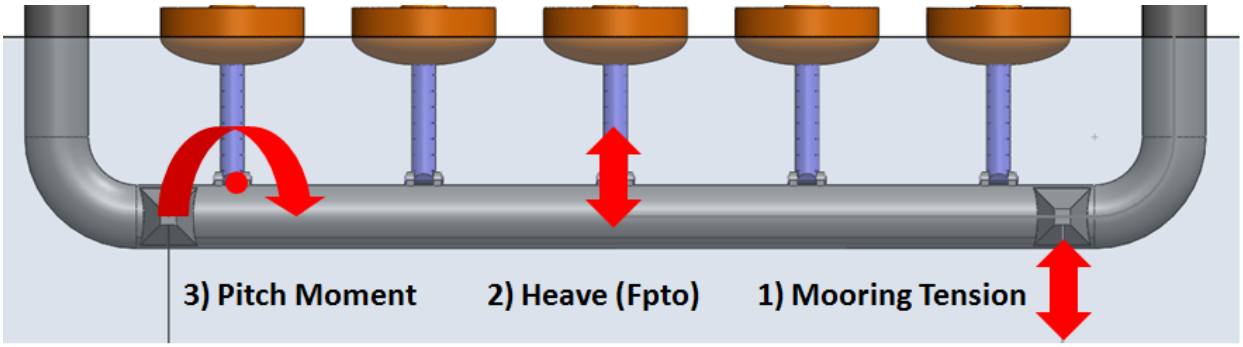

Figure 5.6.5: Visual representation of loads considered.

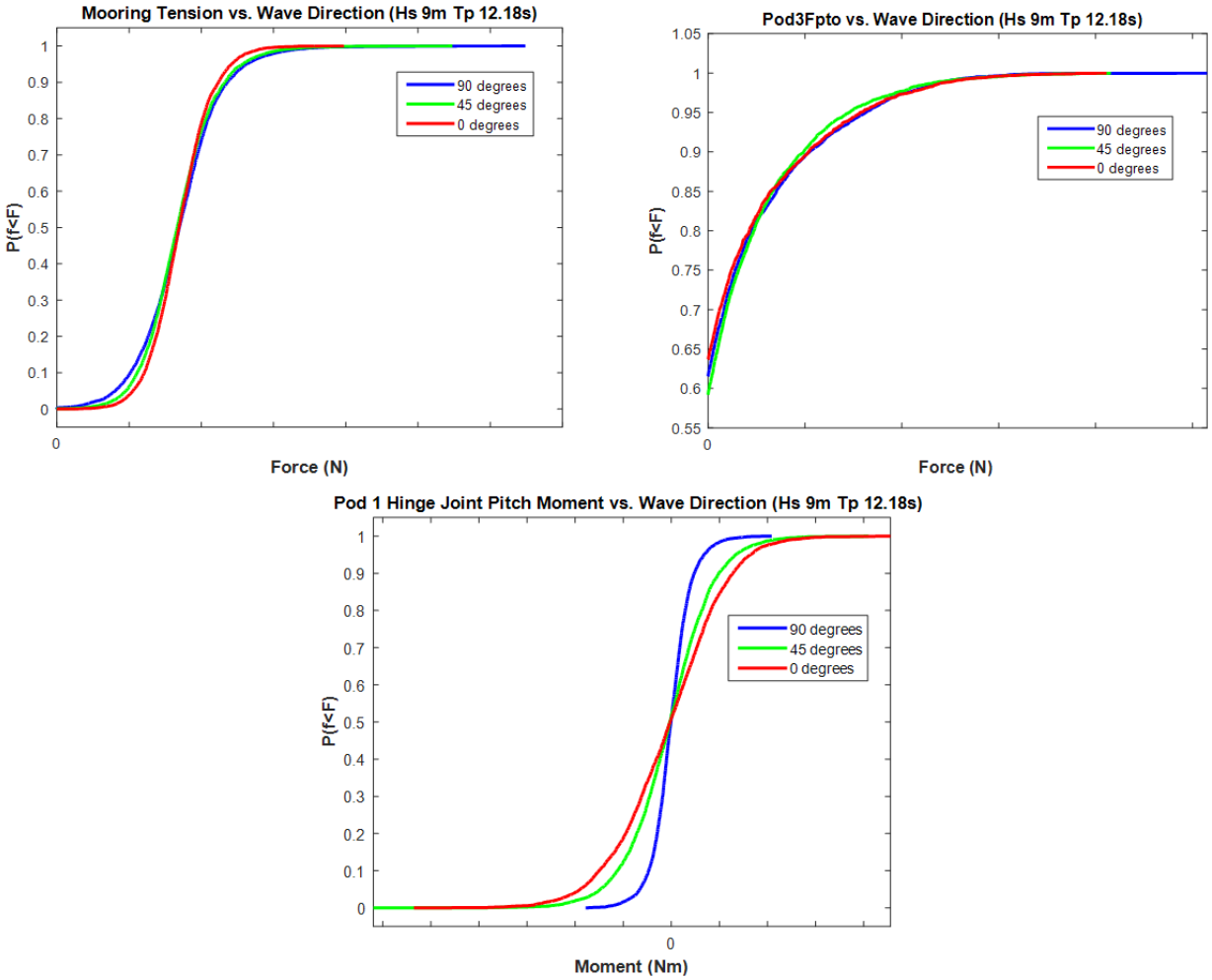

Figure 5.6.6: Non-exceedance plot of:
1) mooring tension for 90, 45 and 0 degree wave directions.
2) Fpto (in heave direction) for 90, 45 and 0 degree wave directions.
3) Pitch moment at Pod 1 hinge joint for 90, 45 and 0 degree wave directions.

Figures 5.6.6 -1 and 5.6.6 -2 show that a wave direction of 90 degrees (incident wave broadside to backbone) results in the highest loads. Meanwhile, Figure 5.6.6 -3 showed the largest

moments on the hinge joint (Pod/Backbone connection) with a 0 degree wave direction. Consequently, the most interesting wave direction to investigate for purposes of extreme loading in the heave direction was the broadside, 90 degree, wave, while 0 degree waves were used to assess extreme loading in the case where pitch direction moments are the load of interest.

Identify the load cases of interest: Using a 90 degree wave direction for heave direction loads and a 0 degree wave direction for pitch moments, each candidate sea state on the shorter period side of the 100 year contour was run.

Significant wave height Hs (m)	5	7	9	11.22
Peak period Tp (s)	5.57	8.76	12.18	17.26

Table 5.6.1: Candidate sea states.

The following figures show the results of each sea state on the load cases of interest (Fpto Pod 3, Mooring line tension, Pitch moment at pod connection).

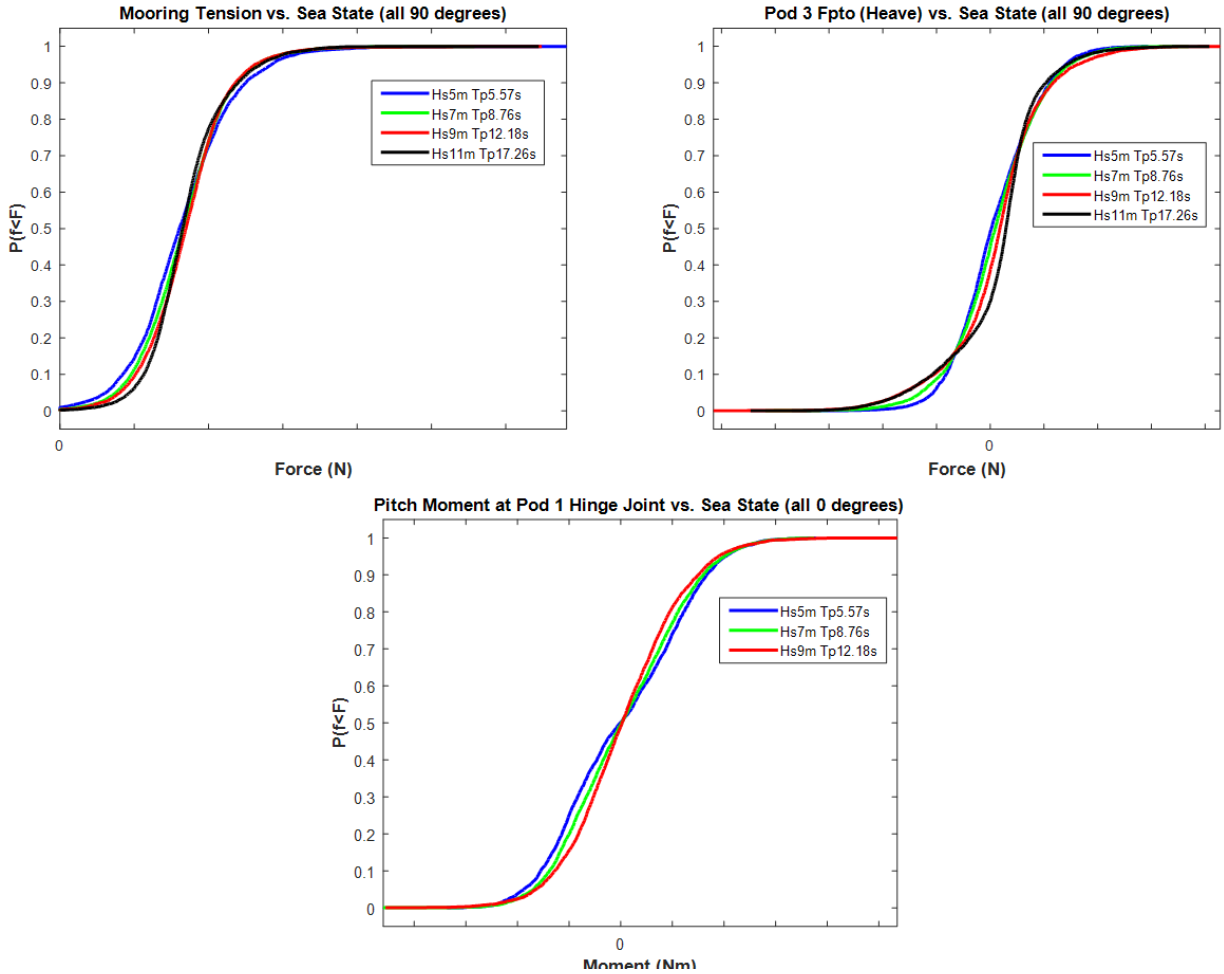

Figure 5.6.7: Non-exceedance plot of:
1) Mooring Tension for Pod 3 for candidate sea states.
2) Fpto for Pod 3 for candidate sea states.
3) Pitch moment at Pod 1 hinge joint for candidate sea

Figure 5.6.7 -1 above shows the non-exceedance of tension in a mooing line of Centipod, which has a pre-tension of approximately $3.3x10^6$ N. The smallest, shortest period sea state, Hs5m, Tp5.57s shows the greatest likelihood of large deviations from the pre-tension as well as the largest individual tensions. This sea state will be of most interest when comparing the effects of MPC and load shedding to baseline.

Of the sea states depicted in Figure 5.6.7 -2, above, Hs9m, Tp12.18s is of most interest. This sea state exhibits both the highest probability of moderate to large loads as well as the largest individual loads.

The moments applied to the pod hinge joint in the pitch direction are shown in Figure 5.6.7 -3 above. The Hs5m, Tp5.57s sea results in a higher probability of moderate loads compared to the larger Hs9m, Tp12.18s sea state. However, the larger sea results in the largest overall moments, and is ultimately of more interest.

5.6.2: Baseline vs MPC

When MPC is applied and the cases of interest are re-run we see a significant reduction in loads. In the case of Fpto Heave force on Pod 3, MPC was run with two tunings, of controller action cost: the operational tune of R = 1e-3 and a "De-Tuned" variant which makes controller action cost one order of magnitude more, R = 1e-2. The results of these runs are shown below.

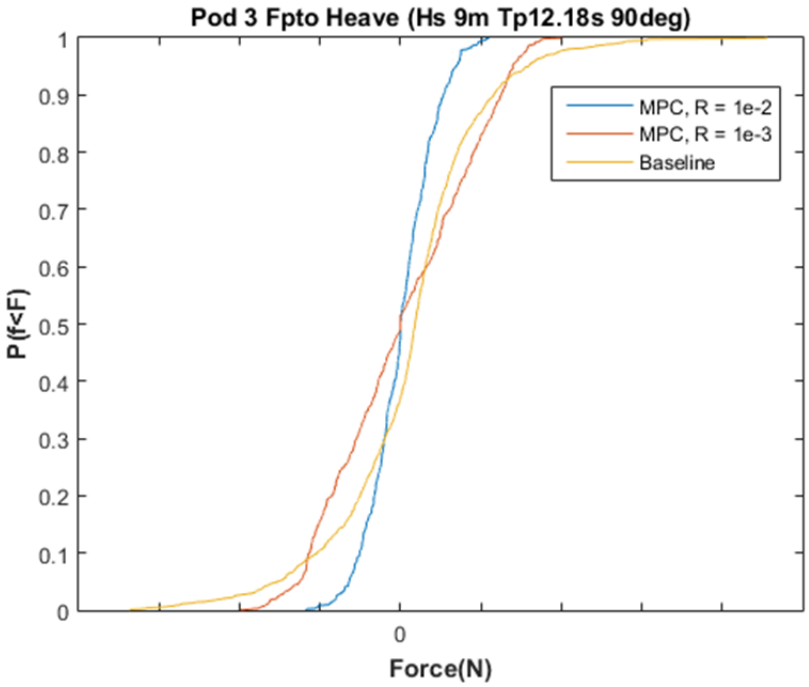

Figure 5.6.12: Pod 3 Fpto non-exceedance plots for baseline and with two tunings of MPC.

As can be seen in Figure 5.6.12, MPC drastically reduces loads. With the operational tune, ultimate loads are reduced approximately 50%, while they are reduced approximately 75% with the "De-Tuned" controller. This shows great promise for the method of controller "De-Tuning".

Of important note with all three methods shown, is the fact that PTO stroke end stops are not applied to this model. Thus, the Pods are free to heave without a position limit, a behavior that is not realistic. In all three cases above, the Pod heaves with amplitude much larger than would typically be allowed in a WEC. This underscores the importance of devoting a much more in-depth study to extreme condition response, which can fully model realistic considerations and utilize high fidelity tools such as CFD. Of particular interest in future work regarding controller use for extreme condition response will be constraint handling. A de-tuned controller may reduce loads on the WEC, but it is less capable of maintaining stroke constraints as well.

Comparisons were also made for the other two loads making up the baseline set.

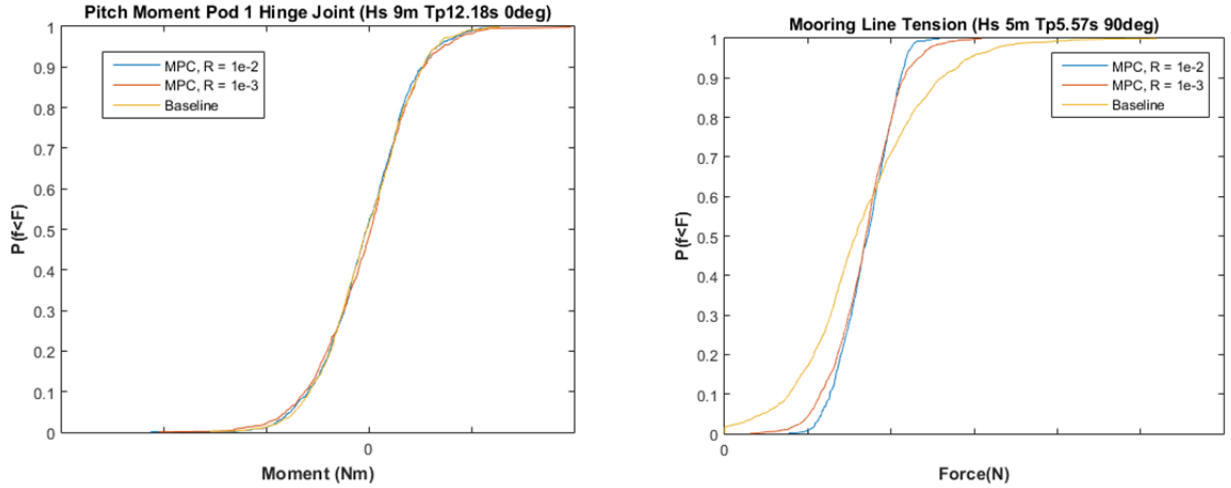

Figure 5.6.13: Non-exceedance plots of baseline and with two tunings of MPC for:
1) Pod 1 Hinge Moment
2) Mooring Line Tension

Figure 5.6.13 -1 shows that the implementation of MPC has little effect on the moments at the Pod's connection point to the backbone compared to the baseline. Meanwhile, in Figure 5.6.13 -2, the impact on mooring tension is similar to that seen in Fpto.

In addition to reducing ultimate loads in the mooring lines, utilization of MPC, and further de-tuned MPC also reduces the chances of slack mooring line conditions. This is critical to reducing the probability of failure in the mooring lines since snap loads are unlikely.

5.7 Task 7.0 - Perform impact analysis

A 161% improvement in AEP was shown to be possible with the implementation of MPC, however, the impact of this performance improvement must be accounted for across the system in order to quantify the performance metrics, and ultimately the LCOE impact.

5.7.1 LCOE

LCOE is calculated with an FCR of 0.108 and the standardized formula of:

$$LCOE = \frac{ICC * FCR + O\&M}{AEP}$$

Where:

ICC – Installed Capital Cost ($)
FCR – Fixed Charge Rate
O&M – Operations & Maintenance ($/yr)
AEP – Annual Energy Production (MWh/yr)

In the above formula, ICC and O&M come from a modified version of the Aug 1, 2014 version of NREL's Cost Breakdown Structure (CBS) template [7]. Meanwhile, the AEP was calculated as described in Sections 5.3 and 5.5.

The CBS holds the cost breakdown of the WEC down to a component level within the machine itself as well as the costs allocated for the balance of system.

5.7.1.1 Cost of the Machine

The cost of the machine itself is largely stable between the baseline and resulting design iterations. With the implementation of the MPC controller, larger operational loads are applied to the structure. Evaluation was required from a structural standpoint to confirm the structural impact of this load increase.

As described in Section 5.5, the increased loads resulting from MPC do not increase the ultimate loads, but rather the magnitude of cyclic loading on the structure. Therefore, the structural impact of MPC is primarily a concern for fatigue analysis. Furthermore, the analysis should focus on the backbone since this serves as the common structure through which all PTO loads are transmitted to the moorings, and it comprises 51% of the WEC's structural mass, making its structural design particularly impactful on overall LCOE.

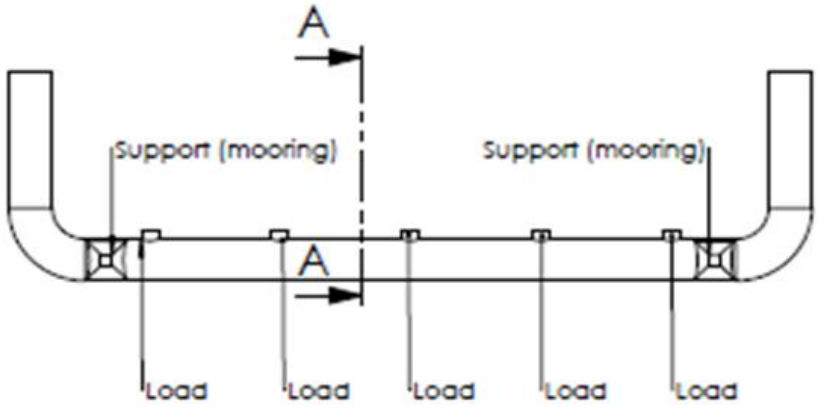

Fig 5.7.1: Backbone Structure

A cumulative damage approach was used to evaluate the loading on the backbone with and without MPC. A loading histogram was produced by recording the peak force of each wave in each 200*Tp time series per sea state. All 190 sea states were multiplied by their occurrence probability in the JPD to reach an annual number of cycles for each load bin.

The loads were then applied to as shown in Figure 5.7.1. Using the cross-sectional geometry parameters of the horizontal span of the backbone, stress was calculated for each load bin creating a histogram of stress magnitude cycles annually for baseline and MPC.

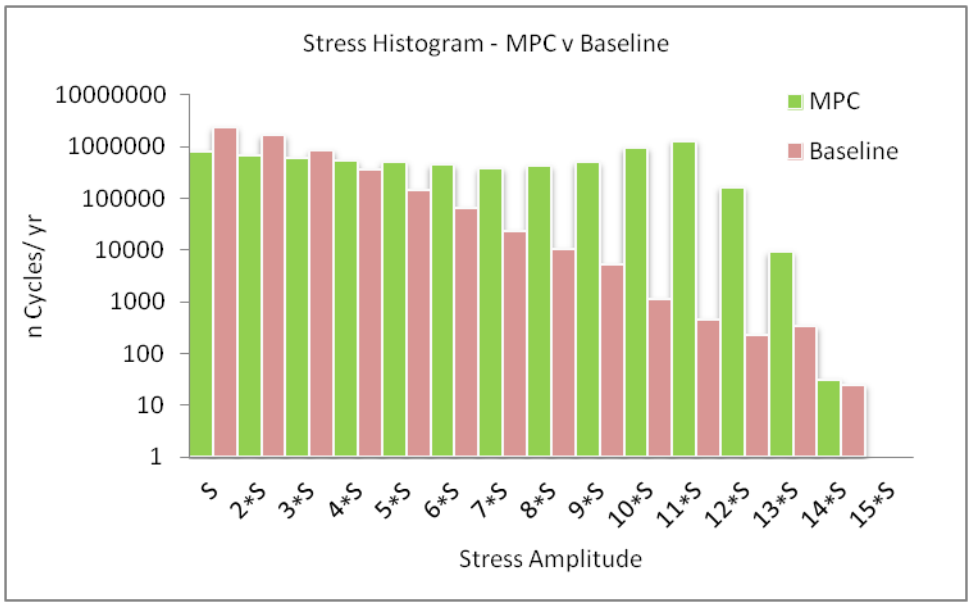

Fig 5.7.2: Stress histogram, MPC vs. Baseline.

Finally, cumulative damage theory was used to evaluate the life of the horizontal span under each of the two loading profiles. The Palmgen/Miner Rule (below) was applied.

$$\sum \frac{n_i}{N_{fi}} = \frac{n_1}{N_{fi}} + \frac{n_2}{N_{f2}} + \ldots\ldots = 1$$

This method calculates the number of cycles allowable for each bucket of the stress histogram summing the buckets together to reach a combined value for life. The number of allowable cycles is a function of stress amplitude as defined by the particular Stess/Number of Cycles (SN) curve.

The SN curve for high strength steel with cathodic protection in seawater was used to evaluate the fatigue life of the base material of the backbone. This SN curve came from the DNV & Carbon Trust Guidelines on Design and Operation of Wave Energy Converters [9].

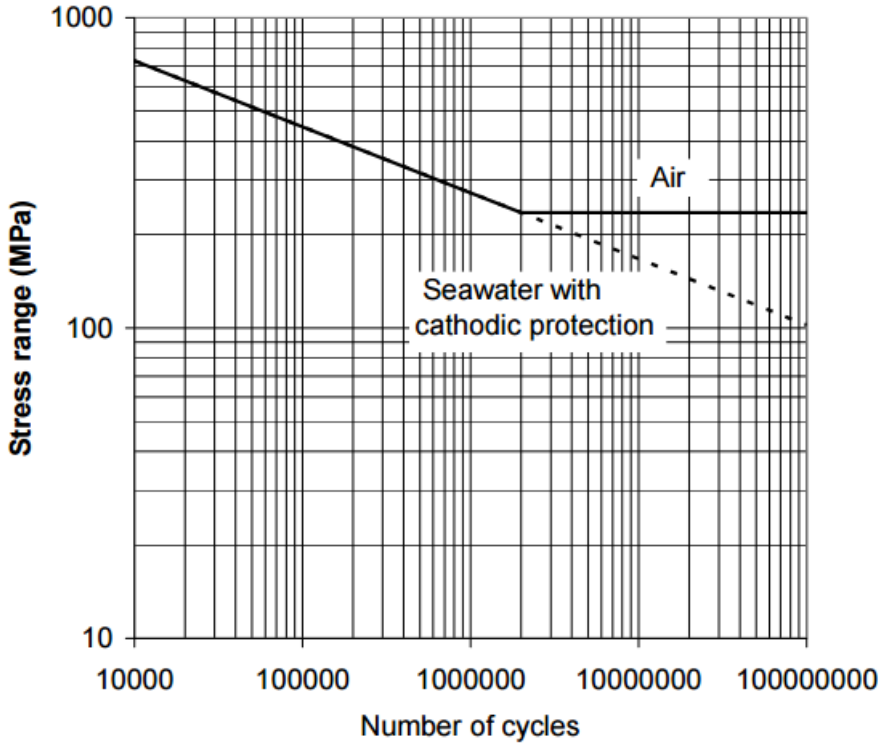

Fig 5.7.3: SN curve for high strength steel with cathodic protection in Seawater [9].

The resulting lifespan of the backbone base material for the MPC load set was well beyond the 20 year design life. Fatigue will need to be continually re-assessed as the structural design matures and greater detail is specified as to potential stress concentrators such as joints and welds. While an important consideration due to the increase in stress amplitude over numerous cycles per year, fatigue was not ultimately a structural design driver in this specific analysis. Therefore, there was no resulting structural impact directly due to the operational loads increase.

The PTO cost was another aspect which needed to be assessed with respect to the WEC capital cost. The PTO required for MPC was scaled up to meet the increased mean and rated power. This project focused on the improvements possible with MPC without the constraints of any specific PTO system. As a result, the PTO has been generalized for this analysis. A cost per kW rated is applied to reach the PTO cost for this CBS. The methodology for this cost is identical to that of the Balance of System costs described in Section 5.7.1.2.

5.7.1.2 Balance of System

The following Balance of System Costs were assessed using industry data on a $/kW basis. The main source of data for this work was *The future potential of wave power in the United States* [8].

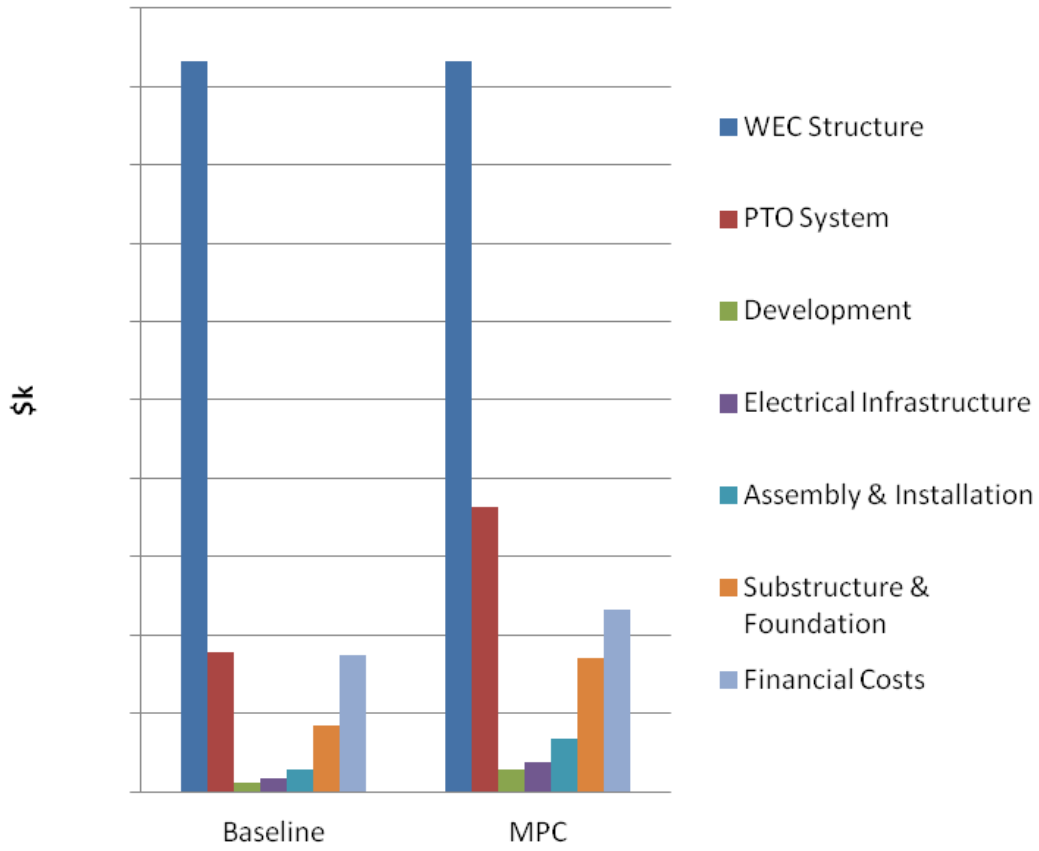

Fig 5.7.4: Balance of System Costs

Development - The development costs include all activities from project inception to financial close, where financial close is the date when project and financing agreements have been signed and all the required conditions have been met.

Electrical Infrastructure - All electrical infrastructure to collect power from generators and deliver to the grid.

Assembly and Installation - Captured within the *Assembly and Installation* category of the cost breakdown was the transport of the WEC and piles to site, installation of piles and the installation of the WEC on its moorings.

Substructure and Foundation - Captured within the *Substructure and Foundation* category of the cost breakdown was the capital expense of the piles and mooring lines themselves.

Financial Costs - Financial costs are comprised of insurance, finance, and contingency costs. These costs are functions of the other capital cost categories, thus an increase in any other capital cost will result in an increase in the financial cost.

5.7.2 AEP

AEP was calculated per the DOE's *Standardized Cost and Performance Reporting for Marine and Hydrokinetic Technologies (2014).* Of most importance in this work is the mechanical power

matrix, which was produced according to specification (i.e. 200*Tp time series simulation of a Bretschneider spectrum for each bin of the resource JPD). It should be noted that the reference resource used in this project is the (Tp-Hs) JPD associated with the 2013 guidance document as this was the most recent at project start and was used throughout for consistency.

5.7.3 PWR

Power to weight ratio (PWR) was calculated on Centipod before and after the implementation of MPC. Mean power increased 161% while the structural mass of Centipod remained constant. The resulting PWR impact was then the calculated using the baseline mass and power, and the MPC mass and power yielding a 161% increase in PWR.

5.7.4 Summary of Metrics

A summary of the System Performance Advancement metrics is shown in Figure 5.7.5 below:

Metric	Proposed Improvement	Achieved Improvement
AEP (MWh/year) Whole Centipod (5 pods) - NorCal resource	95%	161%
LCOE ($/kW-h) 260000MWh/yr array scale at DOE LCOE ref resource	35%	50%
PWR (W/kg) Mean power (W) structural mass (kg)	10%	161%

Fig 5.7.5: System Performance Advancement Metrics Table

The proposed system performance metrics in this project were exceeded by a large margin resulting in an AEP 2.6 larger than baseline, with LCOE cut in half.

5.8 Task 8.0 - Design real-time implementation of MPC controller

The aim of this task was to confirm that the controller created in this project could be run on an embedded micro-controller for practical implementation in a wave energy converter (WEC). Most of the experience with wave energy converters has been in laboratory setting with PC based control or field testing with limited controls capability. Embedded micro-controllers to implement model based controls in wave energy application will require high performance for closed loop control tasks, process control and signal processing, as well as extensive communication protocols. A large memory is required for storing all data safely and in the event of a power failure; critical data should be stored in non-volatile data memory.

Figure 5.8.1: Bachmann MC210 processor module

Embedded micro-controllers have traditionally been limited in CPU speed and memory to implement model predictive control. Limited power and cooling means limited computational resources for computationally intensive numerical optimization with hard real-

time constraints that normally rely on the accuracy of floating-point arithmetic. Embedded controller CPU clock speeds range from 40 MHz to 600 MHz with limited memory. Recent advances in embedded controller have pushed the CPU speeds to 1700 Mh. An example of this is the Bachmann MC210 module that uses Intel Atom processor with clock speed of up to 1.6GHz and a 1GB RAM.

The MPC implementation used a controller time step of 0.5 seconds. The embedded controller needs to be able to carry out the computation at each step faster than the controller time step to be functional for field implementation. Additional tasks such as data acquisition, communication and monitoring will also need to be performed in addition to controller calculation. The scope for the current project was limited to development of model predictive control in simulation and implementation on an embedded controller was not done. In order to evaluate the practicality of implementing this controller on an embedded micro-controller, an alternative method was devised. Real-time implementation of MPC controller was evaluated by simulating the controller on a desktop PC by artificially reducing CPU speed.

To control CPU speed, a tool called BES was used for limiting the CPU speed. BES is a tool that has been developed in the gaming community to limit the CPU usage of certain processes to improve the allocation of CPU to memory and CPU intensive games. BES was used to limit the percent of CPU being used by the MPC controller executable. It is slightly complicated and somewhat inaccurate to benchmark the task based on the clock speed of the CPU on a PC. A PC is performing multiple tasks including running Windows services and other background processes. Fortunately, Windows provides an estimate of the percent CPU usage per task. This was used to evaluate the actual CPU used by the executable and it is assumed that a dedicated processor on an embedded controller will spend 100% processing capacity on calculating the control action.

The simulations were run on a notebook using AMD A6-5350 – 2.9Ghz dual core with 1 GB cache. The MPC controller executable with a simple plant model was run for three different throttle speeds. In the baseline case, with no throttle, the executable used an average of 20% CPU and hence the baseline case can be estimated to be run a 580 Mhz processor. With increasing throttle, the percent CPU used by the executable was reduced increasing the processing time. As can be seen in Table 5.8.1 for a sea state with 8.7s time period and 1.25m significant wave height (Tp: 8s, Hs: 1.25m), the controller worked within the MPC controller time step of 0.5s for CPU speeds greater than 300Mhz. With a 600Mhz processor such as Bachmann MC205 series, the controller will have enough overhead to perform ancillary tasks in addition to solving the model predictive control problem even in high sea state cases where controller may take additional time to solve the optimization problem to avoid exceeding the constraints.

CPU Speed	CPU Time/ Controller step
580 MHz	0.13 s
435 Mhz	0.26 s
290 Mhz	0.52 s

Table 5.8.2: Controller step computational times by CPU speed.

Even though this benchmarking study was not done on an embedded processor, the exercise above demonstrates that the MPC implementation for wave energy converter is very likely feasible on modern embedded controllers. Dehlsen Associates and its partners are continuing to develop this technology and hope to demonstrate the benefits of MPC controller in tank test in the near future using actual hardware.

6.0 Accomplishments

This project proved the merit of MPC from both an AEP and LCOE standpoint, exceeding the performance advancement targets for all project metrics. The LCOE benefit in particular is impactful to the development of Centipod and other WECs, as it shows MPC could be a means of driving the LCOE of Wave Energy Converters down to a competitive level if such control schemes are implemented.

In addition to proving AEP and LCOE advances through this project, another important outcome is the confirmation that implementation of MPC is possible without any upstream sensors. Fe estimation and prediction using only the historical Fpto, velocity, and position time series was achieved in this work. This accomplishment will mean control systems such as this may be easily implemented with existing sensor packages.

7.0 Conclusions

The project showed a 161% improvement in the AEP for the Centipod WEC when utilizing MPC, compared to a baseline, fixed passive damping control strategy. This improvement in AEP was shown to provide a substantial benefit to the WEC's overall Cost of Energy. Furthermore, through the CPU benchmarking work, it has been demonstrated at high level that such a control scheme is implementable in the real world, and will yield substantial performance achievements when tested at scale in real environments.

Being that this work focused on the potential of MPC, and the PTO constraints were relaxed, a challenge facing implementation of the MPC strategy studied in the work is finding a balance between performance improvement and the limitation of constraints applied, such as maximum stroke and PTO force, from an LCOE perspective. Additionally, the development of a Power Take-off (PTO) system capable of providing the necessary reactive power for a reactive control scheme such as MPC will need to be undertaken. These challenges are mild relative to the potential for performance enhancement though the usage of an MPC control scheme, and thus MPC will be pursued into full scale hardware testing by Dehlsen Associates in the continued development of Centipod.

8.0 References

[1] M. Starrett, R. So, T.K.A. Brekken, and A. McCall, “Development of a State Space Model for Wave Energy Conversion Systems,” in IEEE Power and Energy Society , Denver, CO, 2015.

[2] M. Starrett, R. So, T.K.A. Brekken, and A. McCall, “Increasing Power Capture From Multibody Wave Energy Conversion Systems Using Model Predictive Control,” in Technologies for Sustainability (SusTech), 2015 IEEE Conference , Ogden, UT, 2015.

[3] Livingston, M. and Plummer, A. R., “The Design, Simulation and Control of a Wave Energy Converter Power Take Off,” In: 7th International Fluid Power Conference (IFK), Aachen, 2010.

[4] LaBonte, Alison, et al. "Standardized cost and performance reporting for marine and hydrokinetic technologies." Proceedings of the 1st Marine Energy Technology Symposium (METS13), Washington, DC, USA. 2013.

[5] Brodtkorb, Pär Andreas, et al. "WAFO-a Matlab toolbox for analysis of random waves and loads." The Tenth International Offshore and Polar Engineering Conference. International Society of Offshore and Polar Engineers, 2000.

[6] Berg, Jonathan C. "Extreme Ocean Wave Conditions for Northern California Wave Energy Conversion Device" Sandia Natl. Lab. Doc. SAND 9304 (2011): 2011.

[7] MHK LCOE Reporting Guidance Draft. OpenEI. NREL, 1 Aug. 2014. Web. 9 Dec. 2015. ‹ http://en.openei.org/community/document/mhk-lcoe-reporting-guidance-draft ›.

[8] Previsic, Mirko, et al. "The future potential of wave power in the United States." US DOE EERE. August (2012).

[9] DNV "Guidelines on Design and Operation of Wave Energy Converters." Carbon Trust. May (2005).